REVIEW

National Science Review
1: 101–118, 2014
doi: 10.1093/nsr/nwt025

BIOLOGY & BIOCHEMISTRY

Apoptosome and inflammasome: conserved machineries for caspase activation

Jijie Chai and Yigong Shi

ABSTRACT

Apoptosome and inflammasome are multimeric protein complexes that mediate the activation of specific caspases at the onset of apoptosis and inflammation. The central component of apoptosome or inflammasome is a tripartite scaffold protein, exemplified by Apaf-1 and NLRC4, which contains an amino-terminal homotypic interaction motif, a central nucleotide-binding oligomerization domain and a carboxyl-terminal ligand-sensing domain. In the absence of death cue or an inflammatory signal, Apaf-1 or NLRC4 exists in an auto-inhibited, monomeric state, which is stabilized by adenosine diphosphate (ADP). Binding to an apoptosis- or inflammation-inducing ligand, together with replacement of ADP by adenosine triphosphate (ATP), results in the formation of a multimeric apoptosome or inflammasome. The assembled apoptosome and inflammasome serve as dedicated machineries to facilitate the activation of specific caspases. In this review, we describe the structure and functional mechanisms of mammalian inflammasome and apoptosomes from three representative organisms. Emphasis is placed on the molecular mechanism of caspase activation and the shared features of apoptosomes and inflammasomes.

Keywords: apoptosome, inflammasome, caspase activation, apoptosis, inflammation

INTRODUCTION

Apoptosis, also known as programmed cell death, is central to the development and homeostasis of all metazoans [1–3]. Two apoptotic pathways have been documented in cellular and molecular detail: the extrinsic pathway, which is triggered by extracellular death ligands, such as TRAIL and TNF-α, and the intrinsic pathway, which is initiated by intracellular apoptotic stimuli, such as hypoxia and nutrient deprivation (Fig. 1). Apoptosis is executed by the caspases—cysteine proteases with aspartate cleavage specificity in the substrate proteins [4]. Caspases are constitutively synthesized in cells as inactive zymogens and activated at the onset of apoptosis to become mature proteases. Apoptotic caspases comprise two general classes: initiator (or apical) caspase and effector (or executioner) caspase [5] (Fig. 2). Compared to effector caspase, an initiator caspase usually contains a homotypic interaction motif at its amino-terminus, such as a caspase recruitment domain (CARD) or a death effector domain (DED) (Fig. 2). The execution of apoptosis requires sequential activation of the initiator and effector caspases [6,7].

Apoptosis is intertwined with inflammation for pathogen-infected cells. Inflammatory cell death mediated by caspases may serve as an effective defense mechanism against infection. The first cloned caspase is the mammalian interleukin 1β-converting enzyme (ICE) [8,9], later defined as caspase-1 (Fig. 2); caspase-1 plays an important role in inflammation by promoting the maturation of interleukin 1β and interleukin 18. In addition, caspase-1 is involved in triggering an inflammatory form of cell death, named pyroptosis [10,11], which is different from apoptosis and caused by osmotic lysis due to the formation of pores on the plasma membrane. A number of other mammalian caspases, including caspase-4, caspase-5, caspase-11, and caspase-12, have been found to play an important role in inflammation [12] (Fig. 2). The domain organization of an inflammatory caspase is similar to that of an apoptotic initiator caspase, with a CARD at its amino-terminus.

Center for Life Sciences, School of Life Sciences and School of Medicine, Tsinghua University, Beijing 100084, China

E-mails: shi-lab@tsinghua.edu.cn; chaijj@tsinghua.edu.cn

Received 18 September 2013; **Revised** 18 October 2013; **Accepted** 18 October 2013

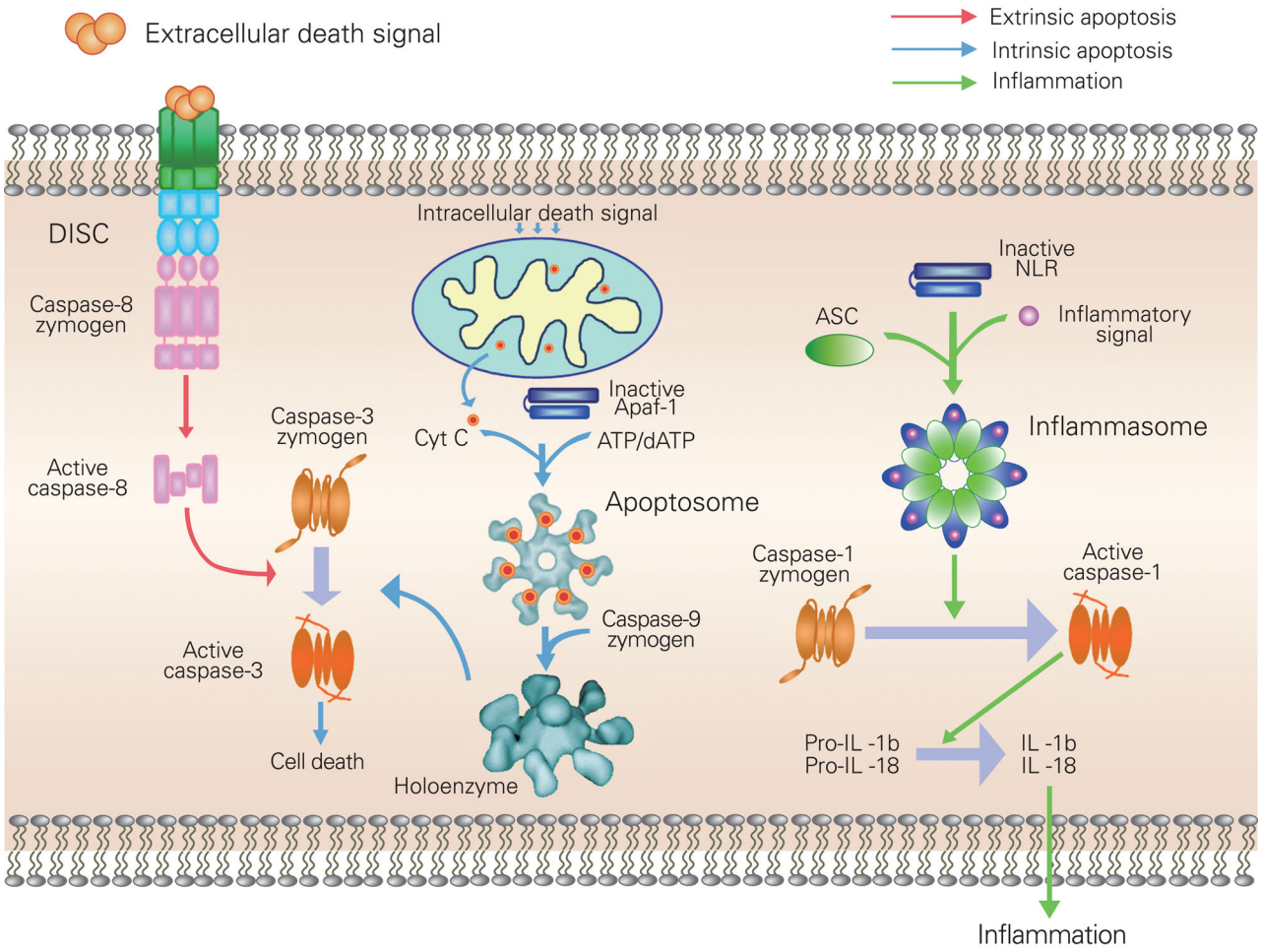

Figure 1. A schematic diagram of the apoptotic and inflammatory pathways. The extrinsic and intrinsic apoptosis pathways are identified by red and blue arrows, respectively. The inflammatory pathway is marked by green arrows. The assembly of a multimeric scaffold protein complex, known as apoptosome or inflammasome, is central to the recruitment and activation of apoptotic initiator caspases or the inflammatory caspases.

An indispensable role for caspase in apoptosis was first documented in the nematode *Caenorhabditis elegans* (*C. elegans*), where the essential gene *ced-3* was found to encode an ICE-like cysteine protease [13,14]. CED-3 was thought to be the only cell-killing caspase in *C. elegans* until the recent discovery of a pro-apoptotic role by the caspase CSP-1 [15]. By contrast, a large number of distinct mammalian caspases have been identified, with 11 from the human genome [5]. In addition to the five inflammatory caspases, at least seven other mammalian caspases have been confirmed to participate in apoptosis. These include four initiator caspases (caspase-2, -8, -9 and -10) and three effector caspases (caspase-3, -6 and -7) (Fig. 2). Notably, some caspases, such as caspase-4, may participate in both apoptosis and inflammation, blurring the demarcation between apoptotic and inflammatory caspases. Of the mammalian initiator caspases, caspase-9 has been rigorously characterized, and its functional homologues have been identified—Dronc in *Drosophila melanogaster* (*Drosophila*) and CED-3 in *C. elegans* (Fig. 2).

CASPASE ACTIVATION

To avoid unwanted cell death or inflammation, all freshly synthesized caspases exist as catalytically inactive zymogens in cells. An effector caspase, such as caspase-3 or -7, is usually activated by an upstream initiator caspase, such as caspase-9, through an aspartate-specific proteolytic cleavage, resulting in the generation of large and small subunits of the mature caspase [5]. As a consequence of the intrachain cleavage, the protease activity of an effector caspase is drastically increased, typically by several orders of magnitude [16]. Once activated, the effector caspases can also cleave and activate other caspases and are responsible for the degradation of numerous cellular targets that eventually lead to cell death.

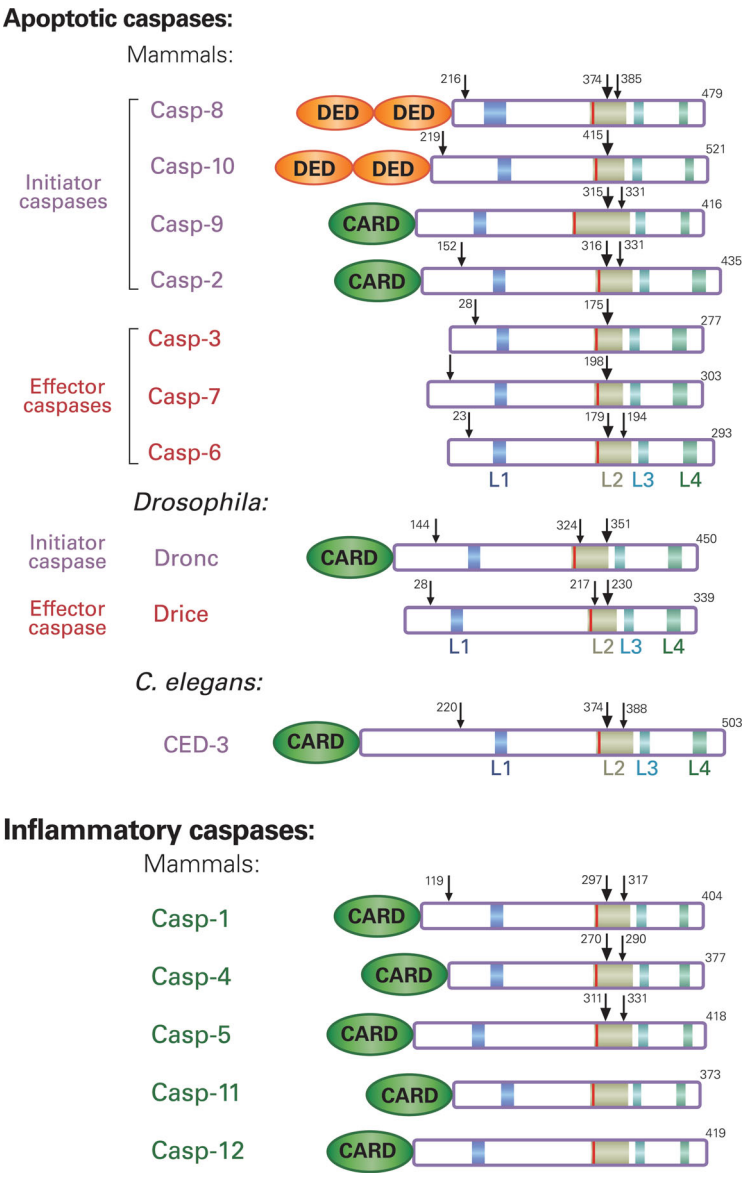

Figure 2. Schematic representation of the apoptotic and inflammatory caspases. These caspases are drawn to scale. The position of the first intra-chain cleavage (between the large and small subunits) is marked by a thick arrow whereas additional cleavages are represented by medium and thin arrows. The CARD and DED are indicated. Apoptotic caspases are shown for mammals, *Drosophila* and *C. elegans*. Notably, caspase-11 is present only in mouse, but not in human.

How does an intra-chain cleavage result in the proteolytic activation of an effector caspase? For all caspases, the catalytic site comprises four essential loops, named L1 through L4. To gain proteolytic activity, the L1–L4 loops must adopt a specific conformation [5] (Fig. 3A). For effector caspases, which are constitutively homo-dimeric, the specific active site conformation of one caspase molecule is critically supported by the L2′ loop of the adjacent molecule through interactions with the L2 and L4 loops [5]. However, for effector caspase zymogens, such as procaspase-7, the L2′ loop of one caspase molecule is covalently restrained and unable to interact with loops L2 and L4 of the neighboring caspase molecule until after the intra-chain cleavage [17,18] (Fig. 3B). Thus, the intra-chain cleavage may allow free movement of the L2′ loop, which subsequently stabilizes the active site conformation of the neighboring caspase molecule (Fig. 3C). Despite strong sequence conservation between caspase-3 and caspase-7, they exhibit quite different intrinsic catalytic activity in their zymogen forms and may undergo distinct pathways to reach the fully activated states [19].

By sharp contrast to the effector caspases, all known initiator caspases are predominantly monomeric in solution. Thus, the formation of the active site conformation in an initiator caspase may require external assistance that is provided by a multimeric scaffold protein complex, dubbed 'apoptosome' for caspase-9 [20] and death-inducing signaling complex (DISC) for caspase-8 [21]. The inflammatory caspase-1 is activated by the inflammasome [22,23]. The ultimate role of the multimeric scaffold protein complex is to help the initiator caspase adopt a productive active site conformation. Previous studies suggest that the intra-chain cleavage is indispensable for the activation of effector caspases, but not for some initiator caspases such as caspase-9 [24,25]. However, in these studies, the protease activity of caspase-3 was measured as an indirect readout of caspase-9 activation. Relying on the direct measurement of caspase-9 activity, recent biochemical characterization shows that the intra-chain cleavage is essential for the apoptosome-mediated stimulation of the protease activity of caspase-9 [26].

THE SCAFFOLD PROTEINS

The major component of the mammalian apoptosome is Apaf-1 that forms a heptameric complex in the presence of cytochrome *c* and ATP/dATP [27]. The Apaf-1 apoptosome physically recruits procaspase-9 zymogen and facilitates its autocatalytic activation [20,28–31]. In *Drosophila*, the activation of the caspase-9 homologue Dronc is mediated by an octameric protein complex of the Apaf-1 homologue Dark [32], also known as Hac-1 [33] or Dapaf-1 [34]. In *C. elegans*, the activation of the CED-3 caspase zymogen is facilitated by the octameric CED-4 complex [35–40]. Both Dark and CED-4 share significant sequence and domain homology with Apaf-1 (Fig. 4). In each case, the scaffold protein complex is generally referred to as apoptosome.

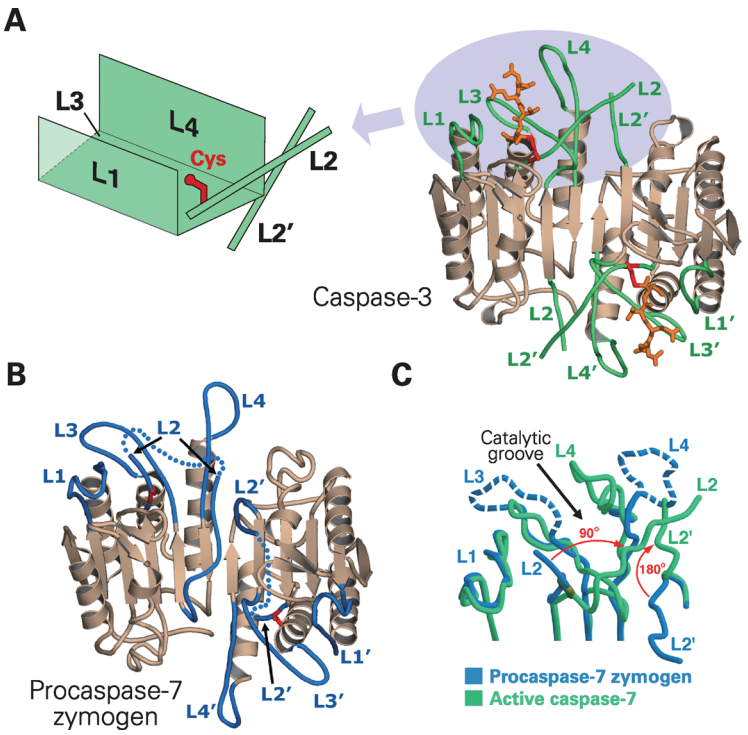

Figure 3. Mechanism of activation for effector caspases. (A) Structural features of an activated caspase-3. The structure of active caspase-3 bound to a covalent peptide inhibitor is shown in the right panel. All known effector caspases are homo-dimeric, with two active sites. The active site of an effector caspase molecule is formed by five loops, four from within (loops L1–L4) and one from the neighboring caspase molecule (loop L2′). The L2′ loop interacts with loops L2 and L4 to stabilize the active site conformation. (B) Structure of the effector caspase-7 zymogen. The L2′ loop is covalently restrained and unable to interact with the L2/L4 loops. Consequently, the active site fails to adopt a productive conformation. (C) Comparison of the active site loop conformations between procaspase-7 zymogen and active caspase-7.

The scaffold protein of caspase-1-activating inflammasome is known as the nucleotide-binding and oligomerization domain (NOD)-like receptor (NLR) (Fig. 4), which senses microorganism-derived pathogen within the intracellular environment. There are 23 NLR family members in the human genome and at least 34 in mouse genome [41,42]. Similar to Apaf-1 and Dark, an NLR exists in an auto-inhibited conformation in its resting state. Relief of the auto-inhibition of the NLR is triggered by binding the inflammatory signal—a pathogen-associated molecular pattern (PAMP) or a host-derived danger-associated molecular pattern (DAMP). Subsequently, through a set of yet-to-be defined processes, NLR oligomerizes and binds the adaptor protein apoptosis-associated speck-like protein containing a CARD (ASC) to form the multimeric inflammasome. ASC in turn recruits procaspase-1 zymogen, leading to its auto-catalytic activation [41,42].

Except NLRP1, Apaf-1, Dark and other NLRs share a conserved tripartite domain organization: an amino-terminal homotypic interaction motif, a central nucleotide binding oligomerization domain (NOD) and a carboxyl-terminal ligand-sensing domain (Fig. 4). The homotypic interaction motifs include CARD, pyrin-like domain (PYD) and baculoviral IAP repeat (BIR). The ligand-sensing domain is represented by leucine-rich repeats (LRRs) in NLRs and two tandem β-propellers, each containing 7–8 WD40 repeats, in Apaf-1 and Dark. NOD is related to the AAA+ ATPases hallmarked by the structurally conserved nucleotide-binding domain (NBD) and belongs to the STAND subfamily [43]. NOD can be further divided into NBD, helical domain 1 (HD1), winged-helix domain (WHD), and helical domain 2 (HD2) (Fig. 4).

There are other scaffold proteins that form multimeric caspase-activating complexes. For example, the activation of caspase-2 in mammalian cells depends on the PIDDosome, which consists of the scaffold protein PIDD and the adaptor protein RAIDD [44], whereas caspase-8 is activated within the DISC [21], which comprises the scaffold FAS and the adaptor FADD. To date, PIDDosome and DISC are yet to be completely reconstituted *in vitro* using purified recombinant proteins. In this review, we focus our discussion on the apoptosomes, involving Apaf-1 and its homologues in *Drosophila* and *C. elegans*, and the inflammasomes.

APAF-1 APOPTOSOME

Discovery and function

The Apaf-1 apoptosome is responsible for the activation of caspase-9, the initiator caspase controlling several forms of intrinsic apoptosis. To date, a great deal has been learned about the function, regulation and three-dimensional structure of caspase-9, Apaf-1 and the Apaf-1 apoptosome [45–47]. Yet the central question of exactly how caspase-9 is activated by the Apaf-1 apoptosome remains largely unknown.

Formation of the Apaf-1 apoptosome involves cytochrome *c*, a molecule that had been known for over half a century to play an essential role in energy production within mitochondria. The remarkable discovery of its crucial role in apoptosis galvanized the entire apoptosis field and exposed the secret life of cytochrome *c* in the cytoplasm just prior to cell death. Cytochrome *c* was first identified as an important cofactor for caspase-3 activation [48] and quickly shown to be an activating ligand for the cellular protein Apaf-1 [49]. In the presence of cytochrome *c* and dATP, Apaf-1 was found to form a stable complex with caspase-9 [50], which then activates caspase-3 and caspase-7.

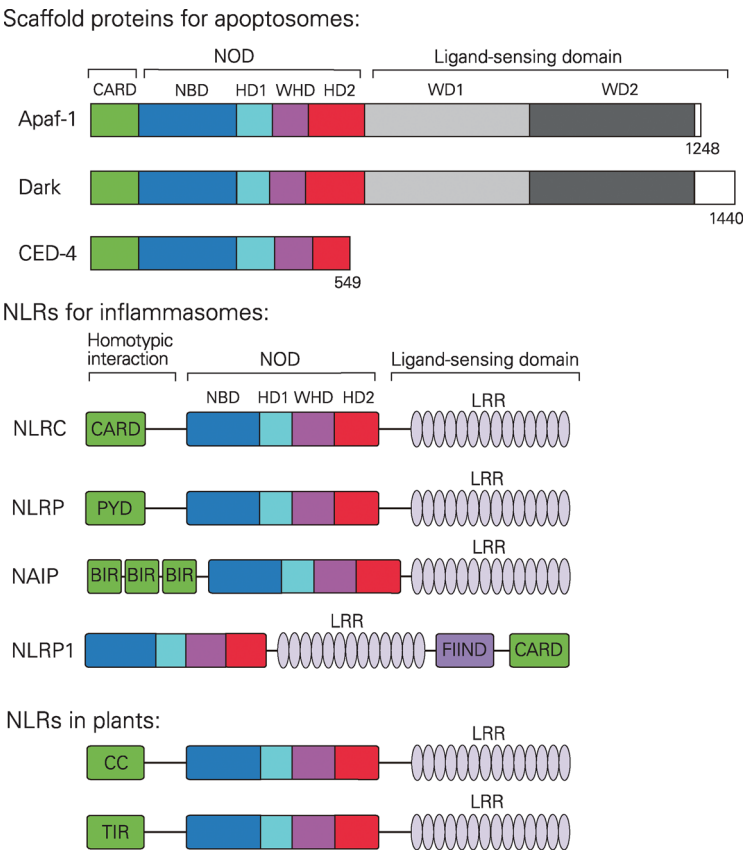

Figure 4. Schematic representation of the scaffold proteins for apoptosomes and inflammasomes. Apaf-1, Dark, and CED-4 are drawn to scale, whereas the NLRs are shown in distinct subfamilies. Notably, while mouse NLRP1s have no PYD, human NLRP1 may harbor a PYD [132]. The various domains are color-coded and labeled. Homotypic interaction motif (CARD, PYD, BIR, CC, TIR): green; NBD, blue; HD1, cyan; WHD, magenta; HD2, red; WD1, gray; WD2, dark gray; cytochrome *c*, yellow; LRR, light purple; FIIND, purple. This coloring scheme is preserved in Figures 5–11 except Figure 6B. Each scaffold protein usually contains a homotypic interaction motif at the amino-terminus, a central NOD, and a ligand-sensing domain at the carboxyl-terminal half. NOD comprises NBD, HD1, WHD, and HD2.

Subsequent investigation revealed that, in the presence of dATP or ATP, Apaf-1 and cytochrome *c* assemble into a multimeric complex of ~1.4 MDa, referred to as the apoptosome [20,28–31]. Apaf-1 CARD directly interacts with the CARD domain of procaspase-9 zymogen, resulting in its recruitment into the Apaf-1 apoptosome, where procaspase-9 undergoes autocatalytic activation [50,51]. Unexpectedly, the fully processed caspase-9 bound to the Apaf-1 apoptosome displays a drastically higher protease activity, typically by 2–3 orders of magnitude, than that of the free, processed caspase-9. This finding constitutes the experimental basis for the holoenzyme concept [30], where the primary function of the Apaf-1 apoptosome was thought to stimulate the protease activity of caspase-9, rather than just to facilitate its autocatalytic cleavage.

Mechanism of Apaf-1 auto-inhibition

Apaf-1 contains three distinct domains, an amino-terminal CARD, a NOD and 14–15 WD40 repeats at its carboxyl-terminal half (Fig. 4A). Apaf-1 directly binds caspase-9 through homotypic interactions involving their respective CARD domains [51]. The NOD is responsible for Apaf-1 oligomerization in the presence of cytochrome *c* and ATP/dATP, whereas the WD40 repeats interact with cytochrome *c*. Apaf-1 has four splicing variants; the two longer variants, each with 15 WD40 repeats, appear to be responsible for the caspase-9 activating function of Apaf-1 [52]. Notably, the NOD contains all the hallmarks of an AAA+ ATPase, and a WD40-deleted Apaf-1 protein exhibits detectable ATPase activity *in vitro* [53].

Prior to cell death stimuli, Apaf-1 exists in an auto-inhibited conformation in normal cells to avoid accidental activation of the procaspase-9 zymogen. Auto-inhibition of Apaf-1 is relieved by binding to cytochrome *c* and replacement of ADP by ATP/dATP. The molecular mechanism by which Apaf-1 maintains its auto-inhibitory state is nicely deciphered by the crystal structures of Apaf-1 [53,54]. Specifically, the role of nucleotide replacement is revealed by the structure of the WD40-deleted Apaf-1 [53], whereas the role of cytochrome *c* binding is inferred from the structural analysis of the full-length Apaf-1 [54].

The structure of the WD40-deleted Apaf-1 reveals a closed, ADP-bound conformation that is maintained by extensive inter-domain interactions among five subdomains: CARD, three-layered α/β domain (or NBD), HD1, WHD and HD2 [53] (Fig. 5A). In this closed conformation, the caspase-9 binding surface in Apaf-1 CARD is partially buried, unavailable for caspase-9 recruitment. This feature explains why Apaf-1 exhibits only weak interactions with caspase-9 in the absence of ATP/dATP or apoptosome formation [50,53]. The deeply buried ADP molecule interacts with three adjoining subdomains to help maintain the closed conformation (Fig. 5A). Due to the buried nature of ADP, its replacement by ATP/dATP, a mandatory step in apoptosome formation, is predicted to require pronounced inter-domain movements in Apaf-1, which may drive the assembly of the caspase-9-activating apoptosome.

The structure of the full-length Apaf-1 reveals an important role for the WD40 repeats in stabilizing the auto-inhibited conformation (Fig. 5B), where three charged amino acids from the 7-bladed β-propeller interact with three complementarily charged residues in NBD and HD2 through hydrogen bonds (H-bonds) [54]. These interactions

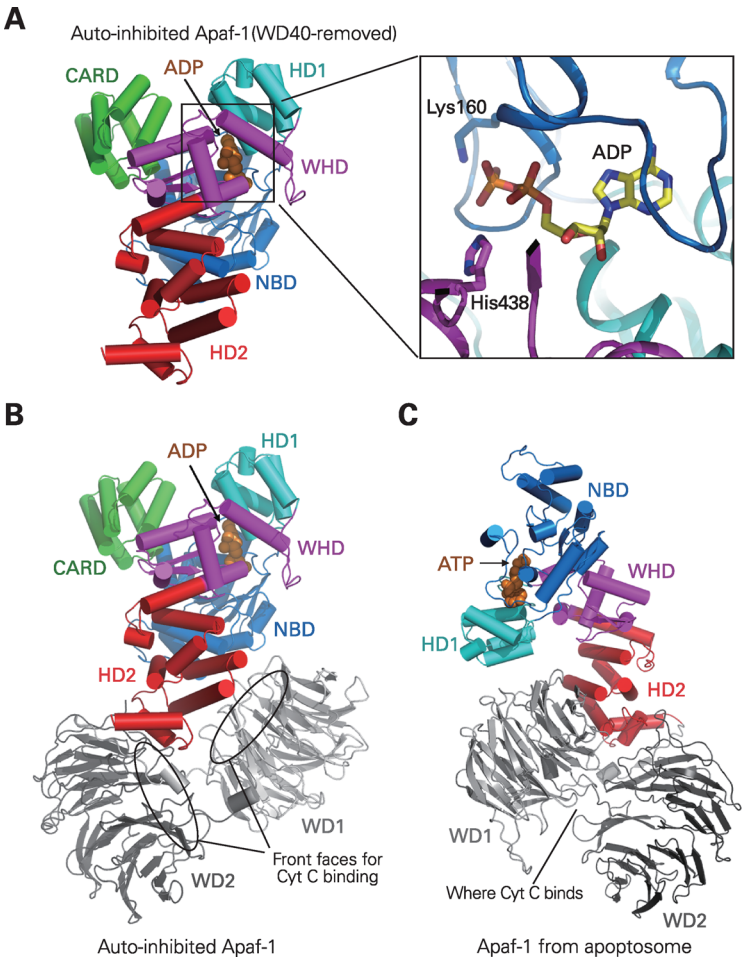

Figure 5. Mechanism of auto-inhibition for Apaf-1. (A) The WD40-deleted Apaf-1 exists in an auto-inhibited state [53]. CARD, NBD, HD1, and WHD closely stack against each other, with the nucleotide ADP buried and bound at the interface among NBD/HD1/WHD. The caspase-9-binding surface on Apaf-1 CARD is partially buried and unavailable for recruitment of caspase-9. (B) The WD40 repeats of Apaf-1 further stabilize the auto-inhibited conformation. Shown here is a composite image of CARD-disordered Apaf-1 structure [54], with CARD modeled on the basis of the WD40-deleted Apaf-1 structure [53]. The first β-propeller directly interacts with NBD through H-bonds. The cytochrome *c* binding surfaces in the two β-propellers are indicated. (C) The activated conformation of Apaf-1. Shown here is a modeled structure of a single full-length Apaf-1 molecule from the assembled Apaf-1 apoptosome. The CARD is not shown because it forms a separate structure with the CARD of caspase-9. All structural figures were prepared using PyMol [133].

further strengthen the extensive inter-domain contacts among CARD, NBD, HD1, WHD and HD2, presumably disfavoring the replacement of ADP by ATP/dATP. These structural features provide a plausible explanation to the observation that the replacement of ADP by ATP/dATP is preceded by cytochrome *c* binding. Cytochrome *c* is sandwiched between two front faces of the two β-propellers [55] (Fig. 5C), which leads to the disruption of the observed interactions between WD40 repeats and NBD/HD2 and facilitates the subsequent replacement of ADP by ATP/dATP. Structural comparison of the auto-inhibited Apaf-1 with that in the apoptosome allows detailed speculation on the conformational changes of Apaf-1 following cytochrome *c* and ATP/dATP binding [54].

CARD plays a key role in maintaining the auto-inhibited conformation of Apaf-1. The extensive interactions between CARD and NBD/WHD, involving 13 H-bonds, are considerably stronger than those between the seven-bladed β-propeller and NBD/HD2 [53,54]. Consistent with the structural observations, the WD40-deleted Apaf-1 only weakly interacts with caspase-9 in the absence of ATP/dATP [53]. In cells, Apaf-1 and caspase-9 only interact with each other in the presence of ATP/dATP and cytochrome *c* [50]. Given the importance of CARD, why is it invisible in the crystal structure of the full-length Apaf-1 [54]? Examination of the Apaf-1 crystal structure [54] reveals that correct positioning of CARD interferes with the formation of the crystal lattice; thus, CARD must be dislodged from its usual position for the crystals to grow. In addition, the non-physiologically high ionic strength in the crystallization buffer (1.4–1.5 M sodium malonate [54]) likely facilitated the displacement of CARD from its usual position. By contrast, the WD40-deleted Apaf-1 was crystallized under considerably milder condition (250 mM sodium chloride [53]). This analysis highlights the importance of cautious interpretation for crystal structures.

Apoptosome formation and regulation

Structure of the Apaf-1 apoptosome, determined by electron cryo-microscopy (cryo-EM), shows a wheel-shaped architecture with 7-fold symmetry [27,56] (Fig. 6A). The NOD constitutes the central hub; the β-propellers form the extended spokes. Recruitment of caspase-9 zymogen to the apoptosome leads to a dome-shaped structure in the center [27]. Improvement of cryo-EM resolution, in conjunction with the atomic structure of Apaf-1 [53], revealed the identity of the dome to be an oligomeric complex of CARDs from Apaf-1 and caspase-9 [55]. Remarkably, a single molecule of caspase-9 was found to be bound in the central hub of the apoptosome, making contacts with NBD and HD1 [57] (Fig. 6B). As will be discussed in detail, this experimental observation provides tantalizing clues about the activation mechanism of caspase-9.

The apoptosome assembly is thought to be quite dynamic. In several studies, the monomeric, auto-inhibited Apaf-1 was found to contain predominantly ADP, not ATP or dATP [53,54,58,59]. The replacement of ADP by ATP/dATP drives the

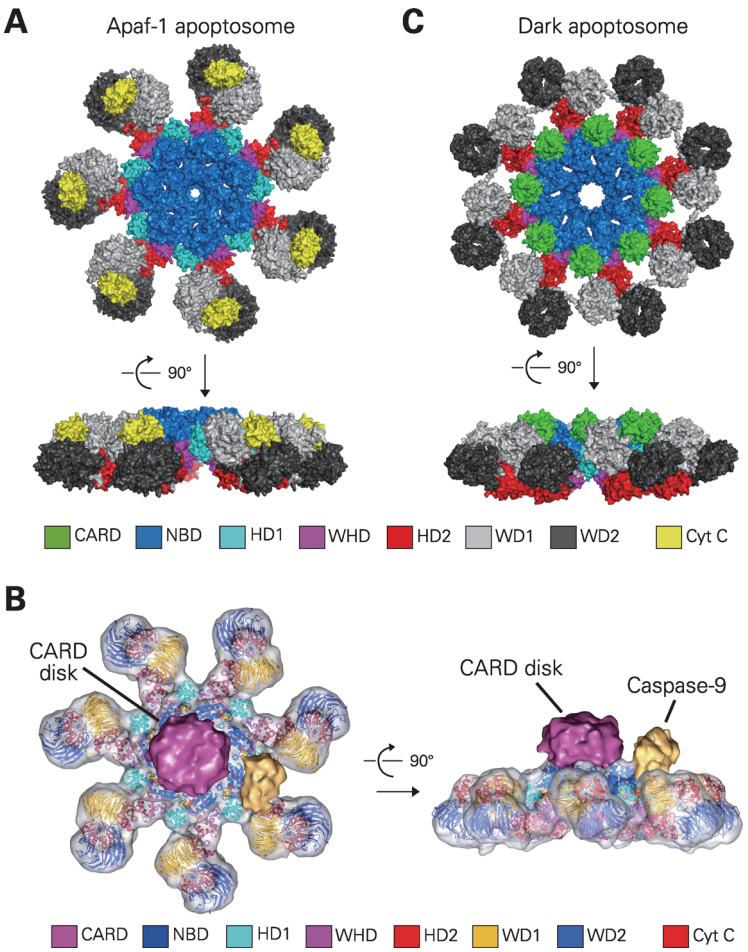

Figure 6. Assembly of apoptosomes in mammals and *Drosophila*. (A) The Apaf-1 apoptosome has a wheel-shaped appearance with 7-fold symmetry [55]. NOD forms the central hub, whereas the cytochrome *c* bound WD40 repeats constitute the spokes. Two perpendicular views are shown here. Following cytochrome *c* binding, assembly of the Apaf-1 apoptosome is triggered by replacement of ADP by ATP or dATP. (B) A single caspase-9 molecule is bound to the central hub of the Apaf-1 apoptosome. Perhaps due to caspase-9 binding, the CARD disk is off center. (C) Structural features of the octameric Dark apoptosome [81]. Unlike the Apaf-1 apoptosome, cytochrome *c* is dispensable for the assembly of the Dark apoptosome. Two perpendicular views are shown here.

apoptosome assembly. As an AAA+ ATPase, Apaf-1 has a low, but detectable, level of catalytic turnover rate [20,53]. We speculate that the ATPase activity of Apaf-1 might be important for the functional regulation of the apoptosome, because ATP hydrolysis likely leads to the disassembly of the apoptosome. In another study [60], Apaf-1 was found to mainly contain dATP and binding to cytochrome *c* triggered hydrolysis of dATP to dADP, which was subsequently replaced by exogenous dATP. Given that recombinant Apaf-1 was used in all cases, it is unclear what contributes to the contrasting observations about the identity of the bound nucleotide in auto-inhibited Apaf-1.

The oncoprotein prothymosin-alpha was thought to inhibit the apoptosome assembly, thus negatively regulating caspase-9 activation [61]. A small molecule alpha-(trichloromethyl)-4-pyridine-ethanol (PETCM) countered prothymosin-alpha mediated inhibition and allowed apoptosome formation [61]. Intriguingly, physiological concentrations of potassium and calcium ions were found to inhibit apoptosome formation and subsequent caspase activation [58,62,63]. In particular, calcium binds to auto-inhibited Apaf-1 and impedes the apoptosome assembly by blocking the exchange of ADP/dADP by ATP/dATP [58]. These findings suggest that the disruption of potassium and calcium homeostasis in cells likely precedes the onset of apoptosome formation and the execution of cell death.

In addition to potassium and calcium ions, multiple intracellular nucleotides at physiological concentrations also appear to guard against cell death by binding to cytochrome *c* and inhibiting the formation of the apoptosome [64]. At concentrations higher than 1 mM, ATP or dATP was also found to negatively regulate apoptosis by binding to and inhibiting caspase-9 [65]. Binding to ATP/dATP by procaspase-9 zymogen or processed caspase-9 results in the marked inhibition of their ability to be activated by the apoptosome [65].

Mechanism of caspase-9 activation

Despite some tantalizing clues and frequent overstatements, the underlying molecular mechanisms by which caspase-9 is activated by the Apaf-1 apoptosome remains poorly understood. The same assessment can be made for just about any other initiator caspase. The central puzzle that remains to be deciphered is: how exactly does a multimeric machinery facilitate the activation of an initiator caspase?

In a general sense, the prevailing model for initiator caspase activation—induced proximity—seems to explain the puzzle already. The initial hypothesis states that the initiator caspases undergo accelerated auto-catalytic processing when brought into the close proximity of each other [16]. The induced proximity model was refined by the proximity-driven dimerization model [66]. Based on this model, the oligomeric apoptosome recruits multiple molecules of inactive caspase zymogen into close proximity of one another, which favors dimerization and hence activation [27,67]. This model, along with other hypotheses, is consistent with the observed second-order activation of caspase-9 by a mini-apoptosome [68].

In a molecular sense, the induced proximity or the proximity-driven dimerization model reveals few mechanistic insights. The observation that high local concentrations facilitate caspase activation has been known for decades. Thus, induced proximity is merely a succinct summary of experimental observations. In addition, the concept that active caspases are dimeric was revealed by the crystal structures of caspase-1 [69,70] and caspase-3 [71] and has been confirmed by just about every caspase crystal structure determined to date. The reason that the dimeric caspase is catalytically active lies in the fact that the L2′ loop from one molecule can conveniently stabilize the active site conformation of a neighboring molecule (Fig. 3). Without the L2′ loop, a dimeric effector caspase is catalytically inactive [17]. The observation that a leucine zipper induced homo-dimer of caspase-9 exhibits drastically enhanced protease activity [72] suggests that the dimerization of caspase-9 may be sufficient for its activation but says little about how caspase-9 is activated within the Apaf-1 apoptosome.

In principle, elucidation of the activation mechanism of caspase-9 requires a detailed structural analysis of the Apaf-1 apoptosome bound to the full-length caspase-9 and structure-guided biochemical characterization. Despite rigorous efforts in the past decade, the atomic structure of the Apaf-1 apoptosome by itself or in complex with caspase-9 has remained elusive. Are the interactions between Apaf-1 and caspase-9 restricted to their respective CARD domains? How many molecules of caspase-9 are recruited into an apoptosome assembly? What is the role of the helical disc formed by the CARD domains in caspase-9 activation? Does the protease domain of caspase-9 physically associate with the Apaf-1 apoptosome? Conclusive answers to these questions are a pre-requisite for understanding the activation mechanism of caspase-9 by the Apaf-1 apoptosome.

After all, the essence of caspase activation is correct positioning of the four active site loops to achieve a proteolytically active conformation. Despite the fact that homo-dimerization is utilized by most caspases to achieve the active conformation, there is little experimental evidence to support such a mechanism for caspase-9 within the apoptosome. The induced conformation hypothesis was proposed to explain the mechanism of initiator caspase activation [73,74]: it stresses the importance of active site conformation, and the recruitment of caspase-9 by the Apaf-1 apoptosome was thought to facilitate the formation of a productive active site conformation. Supporting this hypothesis, an interface-engineered caspase-9, which exists as a constitutive homo–dimer in solution, exhibited a much lower level of catalytic activity compared to the apoptosome-activated caspase-9 [74]. This finding hints at an additional interface between the protease domain of caspase-9 and the Apaf-1 apoptosome. Cryo-EM analysis of the apoptosome holoenzyme reveals such a binding site for a single molecule of the caspase-9 protease domain on the central hub of the apoptosome [57] (Fig. 6B). This observation gives rise to the proximity-induced association model [57], which is similar in nature to the induced conformation hypothesis. Although available experimental evidence supports the possibility that the Apaf-1 apoptosome may employ a strategy other than homo-dimerization to achieve caspase-9 activation, many more experiments need to be performed to scrutinize this hypothesis.

Dark apoptosome in fruit flies

Dronc, the *Drosophila* homolog of mammalian caspase-9, is required for programmed cell death during the normal development of fruit flies [75–77]. An important downstream target of Dronc is the effector caspase Drice, which bears considerable sequence homolog with mammalian caspase-3. Similar to caspase-9, Dronc activation in cells requires the Apaf-1 homolog Dark (also known as Hac-1 or Dapaf-1) [32–34]. However, unlike caspase-9, the N-terminal CARD domain is proteolytically removed in the mature Dronc caspase in *Drosophila* cells [78], suggesting a variation of the activation mechanism compared to caspase-9.

The recombinant, full-length Dark protein exists as a monomer in solution [79]. In contrast to the Apaf-1 apoptosome, the *in vitro* assembly of the Dark apoptosome can be initiated by the presence of dATP, but not by cytochrome *c* [79]. In the absence of exogenous ATP/dATP, the incubation of the monomeric, full-length Dark protein with Dronc zymogen leads to the efficient assembly of an apoptosome complex, within which Dronc zymogen is proteolytically activated (Y Shi, unpublished data). This observation suggests that the Dark apoptosome may be assembled upon encounter with the Dronc zymogen. It is unclear whether the assembly of the Dark apoptosome in cells is triggered by binding to Dronc zymogen or ATP/dATP, or both.

A structural analysis of the Dark apoptosome by cryo-EM revealed two face-to-face assembled, wheel-shaped particles, each involving eight Dark molecules [79] (Fig. 6C). In this initial model, the assignment of individual domains of Dark is different from that for other oligomeric AAA+ ATPases [80]. For example, the CARD domains were placed at the center of the Dark apoptosome to constitute the inner ring [79]. Subsequent cryo-EM analysis at

higher resolution led to the structural revision of the Dark apoptosome, most notably with the placement of the CARD domains on top of the apoptosome disk [81]. The revised Dark apoptosome shares the same set of assembly principles as those for the Apaf-1 apoptosome (Fig. 6A) and the CED-4 apoptosome (to be discussed later).

There are only a few *in vitro* studies on the activation mechanism of Dronc zymogen, but none directly employing the Dark apoptosome [82–84]. Unlike caspase-9, the CARD domain of Dronc is removed from the mature Dronc caspase. Consequently, the mature Dronc caspase is not associated with the Dark apoptosome (Y Shi, unpublished data). Thus, unlike the Apaf-1 apoptosome, the Dark apoptosome appears to only facilitate the auto-catalytic maturation of Dronc zymogen. Compared to the Dronc zymogen, the mature Dronc caspase was reported to exhibit a markedly enhanced catalytic activity [84]; by contrast, Dronc processing was thought to be unnecessary for its catalytic activity [82,83]. Despite these differences, dimerization of Dronc is believed to be the key for its activation. Indeed, the mature Dronc formed a homodimer, whereas the uncleaved Dronc zymogen existed exclusively as a monomer [84]. Thus, the auto-catalytic cleavage in Dronc appears to induce its stable dimerization [83,84], allowing two adjacent protomers to mutually stabilize their active sites. The structural analysis of a CARD-deleted Dronc zymogen revealed an unproductive conformation at the active site, explaining why the zymogen remains catalytically inactive [84].

CED-4 apoptosome for CED-3 activation

Relative to mammals and fruit flies, the apoptotic pathway is simpler in worms. Four genes, *egl-1*, *ced-9*, *ced-4* and *ced-3*, genetically identified in *C. elegans*, control the death of 131 somatic cells during hermaphrodite development [2,85]. CED-3 had long been considered the only cell-killing caspase until CSP-1 was found to promote apoptosis in a subset of cells destined to die during *C. elegans* embryogenesis [15]. Similar to caspase-9 and Dronc, CED-3 exists as an inactive zymogen in cells and undergoes a process of auto-catalytic activation that is mediated by CED-4 [35–40]. In normal cells, the pro-apoptotic CED-4 appears to be sequestered by the mitochondria-bound CED-9 [38,39,86–89], thus unable to activate CED-3. At the onset of cell death, the BH3-only protein EGL-1 is transcriptionally activated and unleashes the pro-apoptotic activity of CED-4 by disrupting the CED-4-CED-9 complex [90–93]. The released CED-4 is thought to form an oligomeric apoptosome, that then facilitates the activation of CED-3 [40].

Biochemical and structural investigations have provided significant mechanistic insights into the interplay among EGL-1, CED-9, CED-4, and CED-3. Only the oligomeric CED-4 apoptosome, but not the monomeric or homo-dimeric form of CED-4, is capable of activating the CED-3 zymogen [94]. Atomic structure of a CED-4-CED-9 complex revealed that one molecule of CED-9 sequesters CED-4 in its homo-dimeric form through extensive interactions, thus blocking formation of the CED-4 apoptosome [94,95] (Fig. 7A). Thus, unlike auto-inhibition for Apaf-1, CED-4 at the resting state is inhibited by CED-9 binding. How does EGL-1 counter CED-9-mediated sequestration of CED-4? EGL-1 and CED-4 bind to two non-overlapping sites on the surface of CED-9; however, the overall CED-9 conformation required for CED-4 binding is quite different from that required for EGL-1 binding. The binding affinity between CED-9 and EGL-1 is considerably higher than that between CED-9 and CED-4; consequently, EGL-1 is able to interact with CED-4-associated CED-9 [94,95]. Binding to EGL-1 induces allosteric changes in CED-9, leading to the dissociation of CED-9 from the CED-4 dimer [94,96]. The freed CED-4 dimer further oligomerizes to form a CED-4 apoptosome.

The crystal structure of the CED-4 apoptosome reveals a funnel-shaped architecture, with eight molecules of CED-4 organized as a tetramer of an asymmetric dimer [97] (Fig. 7B). The basic unit—asymmetric dimer of CED-4—is exactly what is sequestered by CED-9. Thus, unlike Apaf-1 or NLR, CED-4 in the resting state already exists in an activated conformation, except that the interface required for apoptosome formation is blocked by CED-9 [97]. Similar to caspase-9, the mature CED-3 protease is predominantly monomeric in solution and forms an active holoenzyme with the CED-4 apoptosome, within which the protease activity of CED-3 is markedly stimulated [97]. Unexpectedly, the octameric CED-4 apoptosome appears to bind only two, not eight, molecules of mature CED-3. The EM analysis of the CED-3-CED-4 holoenzyme strongly suggests that the two CED-3 molecules may be bound within the hutch of the funnel-shaped CED-4 apoptosome [97].

The L2′ loop of CED-3 was recently found to play a major role in the formation of an active CED-4-CED-3 holoenzyme [98]. The crystal structure of the CED-4 apoptosome bound to the L2′ loop fragment of CED-3 reveals specific interactions between a stretch of five hydrophobic amino acids from CED-3 and a shallow surface pocket within the hutch of the funnel-shaped CED-4 apoptosome.

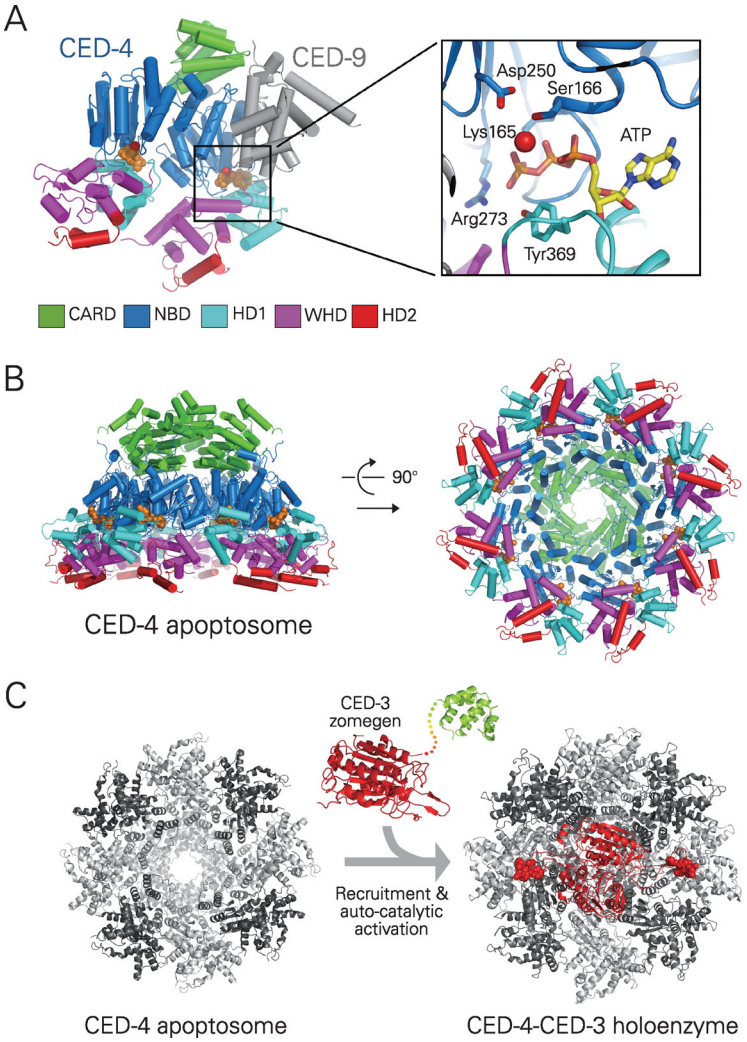

Figure 7. Assembly of the CED-4 apoptosome in *C. elegans*. (A) CED-9 sequesters an asymmetric dimer of CED-4 [94]. Unlike Apaf-1 or Dark, CED-4 exists in a constitutively active conformation, with ATP bound at the interface between NBD and HD1. However, CED-9 binding prevents the CED-4 homo-dimer from oligomerization. (B) The CED-4 apoptosome has a funnel-shaped appearance and contains eight molecules of CED-4 [97]. Assembly of the CED-4 apoptosome is initiated by displacement of CED-9 by EGL-1 from the CED-4–CED-9 complex. (C) The CED-3 zymogen is thought to be recruited into the hutch of the funnel-shaped CED-4 apoptosome, where CED-3 undergoes auto-catalytic activation. The freed CED-4 dimer further oligomerizes to form the CED-4 apoptosome.

Structure-guided biochemical analysis confirms the functional importance of the observed CED-4–CED-3 interface [98]. Structural analysis, in conjunction with published evidence, strongly suggests a working model, in which two molecules of CED-3 zymogen, through specific recognition, are forced into the hutch of the CED-4 apoptosome, consequently undergoing dimerization and auto-catalytic maturation (Fig. 7C). Although how exactly two CED-3 molecules are bound and forced to dimerize within the CED-4 apoptosome remains to be characterized, the available experimental observations are consistent with the induced conformation model [73,74], or the proximity-driven association model [57]. This mechanism represents a major refinement of the induced proximity model for initiator caspase activation.

AUTO-INHIBITION OF NLR

Most of the inflammasomes described to date contain an NLR scaffold protein, such as NLRP1, NLRP3 and NLRC4 (NOD-, LRR- and CARD-containing 4; also known as IPAF or Card12) (Fig. 4). NLRC4 contains an amino-terminal CARD, an NOD and LRRs at the carboxyl-terminal half. The crystal structure of the mouse CARD-deleted Nlrc4 reveals an auto-inhibited conformation [99] (Fig. 8A). Similar to Apaf-1, the auto-inhibition of Nlrc4 is partly achieved by inter-domain interactions among NBD, HD1, WHD and HD2, which is stabilized by a bound ADP molecule. Notably, the relative domain organization among NBD/HD1/WHD is the same between Apaf-1 and Nlrc4 (Fig. 8A, B), further supporting a conserved mechanism of auto-inhibition.

Despite low sequence homology, the NBD of Nlrc4 is structurally similar to that in CED-4 (which represents the activated form) [97]. However, relative to NBD, the WHD in Nlrc4 is located in a strikingly different position compared to CED-4 (Fig. 8A), suggesting that the activation of NLR mainly involves the structural re-organization of its WHD relative to NBD. This is supported by cryo-EM studies of the Apaf-1 and Dark apoptosomes [55,81]. The HD2 of Nlrc4 that packs against one side of the NBD is positioned similarly as the WHD of CED-4, suggesting that the HD2 may have a role in Nlrc4 auto-inhibition. In agreement with the structural analysis, mutations of the amino acids critically involved in the HD2-NBD interactions resulted in a constitutively active Nlrc4, which induced processing of IL-1β in a ligand-independent manner [99].

Structural comparison of Nlrc4 with a CED-4 dimer provides additional insights into the mechanism of NLR auto-inhibition by its carboxyl-terminal sensor domain. When superimposed with one molecule of a CED-4 dimer, the LRR domain of Nlrc4 overlaps with the other CED-4 molecule, suggesting that the LRR may also play a key role in sequestering Nlrc4 in a monomeric state. Indeed, Nlrc4 mutants with either LRR deleted or the LRR-NBD interaction compromised constitutively activated the processing of IL-1β [99–101]. The LRR-mediated Nlrc4 inhibition is reminiscent of CED-4 inhibition by CED-9 in which CED-9 blocks CED-4 oligomerization by blocking

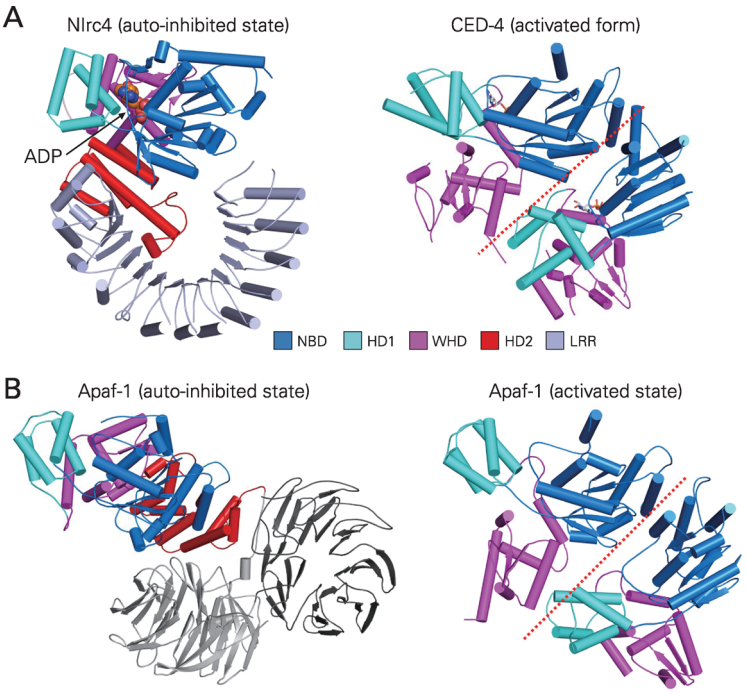

Figure 8. Mechanism of auto-inhibition for Nlrc4. (A) Structural comparison of the auto-inhibited Nlrc4 with activated CED-4. Overall structure of the auto-inhibited Nlrc4 (residues 90–1024) is shown in the left panel [99]. Two neighboring CED-4 molecules from the CED-4 apoptosome are shown in the right panel. The interface between the two CED-4 molecules is indicated by a red dashed line. The NBD-HD1 domains of the CED-4 molecule to the top left were aligned with the corresponding domains of Nlrc4. (B) Structural comparison of the auto-inhibited Apaf-1 with activated Apaf-1. Left panel: Overall structure of auto-inhibited Apaf-1 (residues 105–1248) [54]. Right panel: Two neighboring Apaf-1 molecules from the Apaf-1 apoptosome [55].

the CED-4 interface that is required for oligomerization [97] (Fig. 7A). Notably, when placed into the Apaf-1 apoptosome based on NOD, the carboxyl-terminal β-propeller in the auto-inhibited Apaf-1 overlaps with an adjacent Apaf-1 molecule (Fig. 8B). Thus, in addition to contributing to the stability of the locked conformation in NOD, the WD40 repeats sterically occlude the monomeric Apaf-1 from oligomerization. The HD2- and LRR-mediated auto-inhibition of Nlrc4 appears to be additive, because an Nlrc4 variant carrying the Y617A and G520Y mutations predicted to perturb the NBD-HD2 and NBD-LRR interaction, respectively, is more efficient for ligand-independent IL-1β activation than either mutation alone [99]. Given the highly conserved structural organization, the mechanism of auto-inhibition by Nlrc4 may hold true for other NLRs.

NLR ACTIVATION AND FORMATION OF INFLAMMASOME

NLR proteins are thought to function as binary molecular switches, with the ADP-bound form corresponding to the monomeric 'off' state and the ATP-bound form to the oligomeric 'on' state [102]. Indeed, ADP was bound in the auto-inhibited forms of Nlrc4 [99] and Apaf-1 [53,54], whereas ATP is present in the activated form of CED-4 [94]. In both Nlrc4 and Apaf-1, ADP is buried at the interface formed by NBD, HD1 and WHD. Except His438 of Apaf-1 or His443 of Nlrc4 (both from WHD), all the amino acids involved in recognition of ADP are from NBD and HD1, and many of them, in particular those from the P loop, are conserved among Apaf-1, Nlrc4 and other AAA+ ATPases [103]. His438 of Apaf-1 and His443 of Nlrc4, however, are uniquely conserved in Apaf-1 and NLRs from both mammals and plants (Fig. 9A).

The mutation H443L in Nlrc4 resulted in the constitutive activation of Nlrc4 in HEK293 cells, independent of protein concentration [99]. Notably, there is only one H-bond from WHD to ADP, mediated by His443 (Fig. 9B). As mentioned above, WHDs of Apaf-1 and DARK undergo substantial structural rearrangement with respect to NBD following their activation. A similar conformational change is also expected for the auto-inhibited Nlrc4 upon activation. Thus, the H-bond between ADP and His443 may be exclusively present in the auto-inhibited Nlrc4. For this reason, we propose His443 in Nlrc4 (or His438 in Apaf-1) to be an 'ADP sensor' (Fig. 9A). Disruption of the unique H-bond would favor conformational changes in the WHD of the auto-inhibited Nlrc4. As normal cells contain 5–10-fold more ATP than ADP, a compromised ADP–Nlrc4 interaction by the H443L mutation favors ATP binding. The impact of H443L is reminiscent of GTPase activation by guanine nucleotide exchange factors [104]. His443 is located in the MHD motif; the mutation of Met or His in the 'MHD' motif results in the constitutive activation of the receptors [105–108]. Intriguingly, while invariant in plant NLRs, His443 is absent in 5 out of the 23 human NLRs. It is unclear whether any amino acid from the WHD of these NLRs is involved in the interaction with ADP.

Compared to apoptosomes, there is scant structural information on the inflammasomes. Electron micrograph studies of the NLRP1 and NAIP/NLRC4 infammasomes suggest that the assembly of the inflammasome may share the same set of principles as the formation of the apoptosome. Both NLRP1 [109] and NAIP/NLRC4 [110] inflammasomes have a disk-like structure, generally similar to that of the apoptosomes. The NLRP1 inflammasome is likely to be a heptamer, whereas the NAIP/NLRC4 inflammasome appears to contain 11 or 12 protomers with one or two NAIP5 molecules (Fig. 9C). Incorporation of more

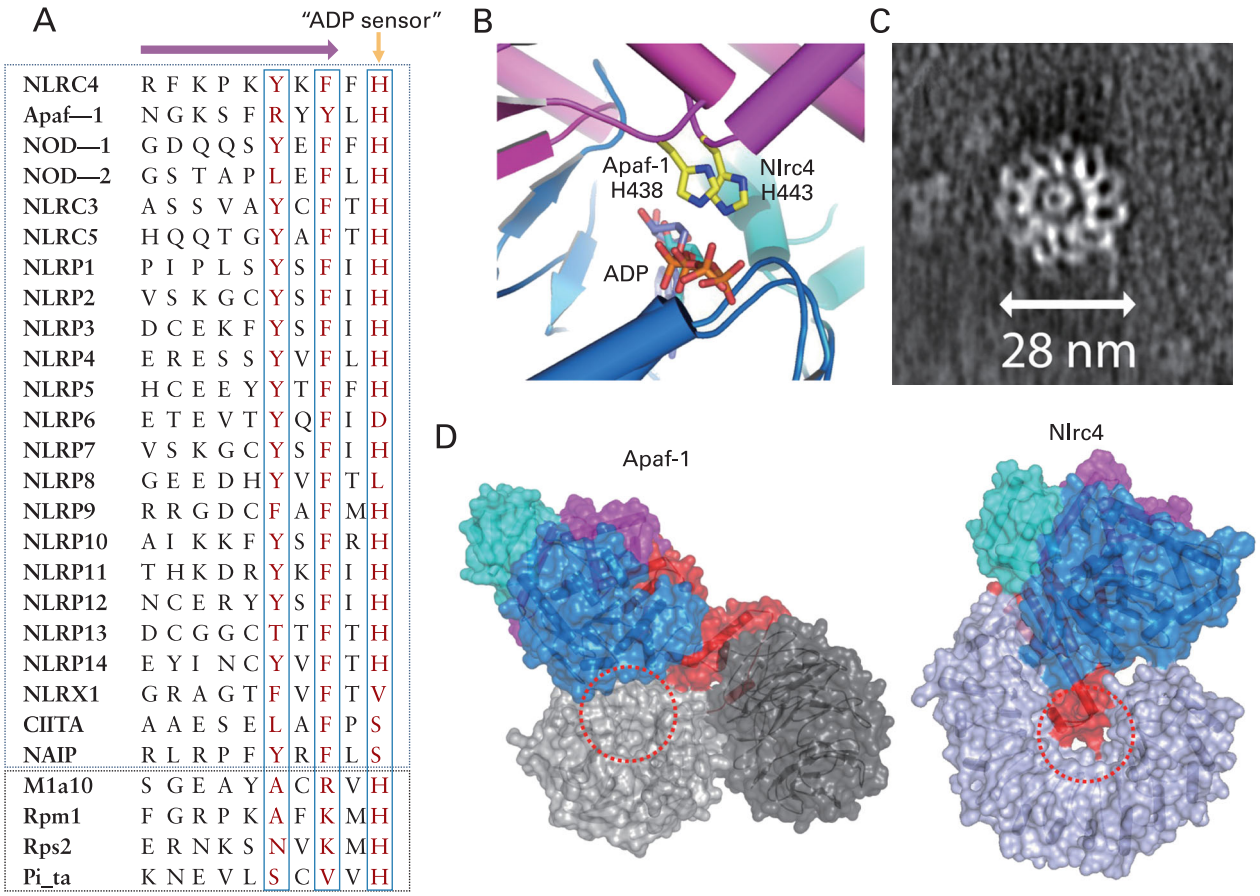

Figure 9. Activation mechanism of NLRs. (A) Most NLR proteins have a conserved histidine residue as the ADP sensor. This histidine, His443 in Nlrc4 and His438 in Apaf-1, is located in the WHD and makes a H-bond to ADP. (B) The ADP sensor is the only residue that coordinates ADP but is not from the NBD or HD1 domains in Nlrc4 and Apaf-1. Shown here is structural overlay of Nlrc4 [99] and Apaf-1 [53] around the ADP binding site. Most of the ADP-coordinating residues from NBD and HD1 are omitted for clarity. (C) An electron micrograph of the NAIP5-NLRC4 inflammasome. The NAIP-NLRC4 inflammasome shares a similar set of structural features as the apoptosomes. The image was adapted from a published study [110]. (D) A putative ligand-binding groove in Nlrc4 resembles the cytochrome *c* binding site in Apaf-1. Shown here are structures of auto-inhibited Apaf-1 (left) and Nlrc4 (right). The regions identified by red circles indicate a cytochrome *c* binding site in Apaf-1 and a putative ligand-binding groove in Nlrc4.

NAIP5 molecules into the inflammasome is thought to be unfavorable for caspase-1 activation, because the CARDs of NLRC4, thought to be important for pro-caspoase-1 recruitment, may be occupied by NAIP5. It is unclear how NAIP5 induces NLRC4 oligomerization.

In the Apaf-1 apoptosome, the cytochrome *c* binding site is located far away from WHD [55]. Structural comparison of Apaf-1 in auto-inhibited and activated forms reveals striking rearrangement of the first β-propeller relative to the combined rigid block of WHD, HD2 and second β-propeller during activation. Thus, the binding of cytochrome *c* results in the swinging of the first β-propeller out of its resting position (Fig. 9D, left panel), thereby releasing its attachment to NBD [54]. In addition, cytochrome *c* binding may induce conformational changes in the first β-propeller, which may also perturb the neighboring domains, such as NBD, HD2 or the second β-propeller. Because HD2 and WHD remain as a rigid body during activation, any perturbation in HD2 can be relayed to WHD and adversely affect the H-bond between His438 and ADP. This would facilitate the exchange of ADP by ATP and Apaf-1 activation. Interestingly, similar to the cytochrome *c* binding site in Apaf-1, a surface groove is present between the central inner surface of the LRR solenoid and HD2/NBD in Nlrc4 (Fig. 9D, right panel). Upstream ligand may bind to this site and induces Nlrc4 activation through a mechanism similar to that for Apaf-1.

DISEASE-ASSOCIATED MUTATIONS IN NLR

Compared to the inflammasomes formed by NLRC4, NLRP1 and other known NLRs, the

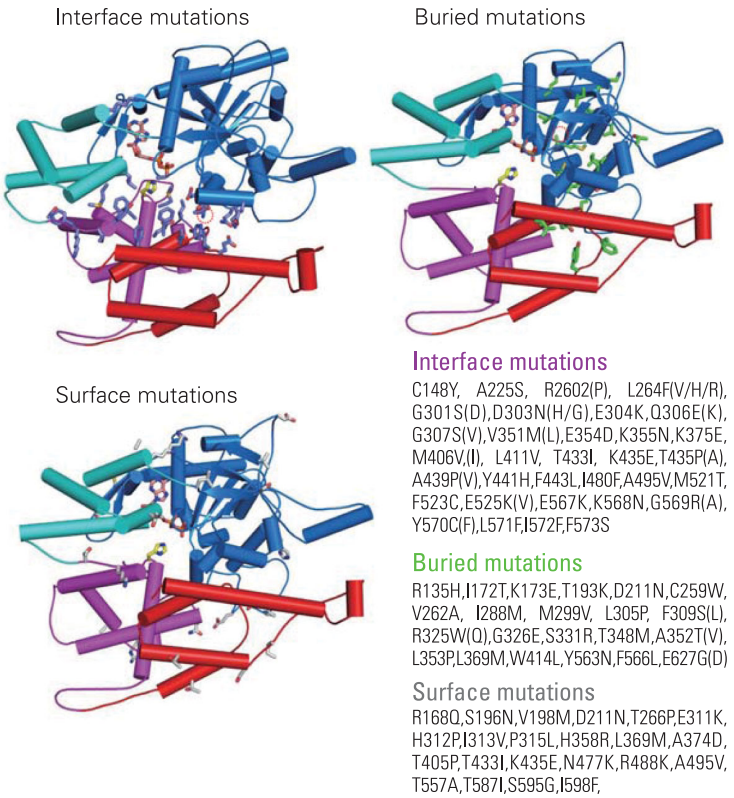

Figure 10. Mapping of disease-associated mutations on a modeled structure of NLRP3 NOD. The structure of human NLRP3 (residues 90–650) shown was predicted using the program ROBETTA (http://robetta.bakerlab.org/index.html). The model was constructed using the structure of Nlrc4 (PDB code: 4KFX) as the template. The disease mutations were taken from the database (http://fmf.igh.cnrs.fr/ISSAID/infevers/index.php). Criteria for grouping of the mutations: mutation of a residue located at the NBD-WDH or NBD-HD2 interface belongs to "Interface mutations"; mutation of a solvent-inaccessible or structural residue belongs to "Buried mutations"; all the others belong to "surface mutations".

NLRP3 inflammasome can be activated by a much wider range of stimuli including microorganisms, endogenous danger signals and environmental irritants [111–113]. However, no direct interaction between any of these activators and NLRP3 has been demonstrated, suggesting that NLRP3 is unlikely to recognize these activators directly. Several models for the activation of the NLRP3 inflammasome have been proposed, involving factors, such as potassium efflux, generation of reactive oxygen species (ROS) and lysosomal destabilization [114]. Recent studies revealed an essential role for mitochondria in NLRP3 inflammasome activation [115–118]. Although the precise activation mechanisms for NLRP3 inflammasome remain to be defined, the mechanism of auto-inhibition for NLRP3 is thought to be similar to that for NLRC4 due to their conserved structural organization and sequence features.

Mutations in NLR have been associated with human inflammatory disorders [41,119,120]. For instance, many disease-derived mutations have been reported for NLRP3 (Cryopyrin/NALP3) [121–124] and most of them map to the central NOD encoded by exon 3, with a few in LRR. The mutations that cause abnormal activation of NLRP3 are thought to contribute to the Cryopyrin/NALP3-associated periodic syndromes (CAPS) [124,125], which feature skin rashes and prolonged episodes of fever without apparent infection [126]. The mechanism by which the CAPS mutations cause diseases is poorly understood. *In vitro* studies showed that the disease-associated mutations enhance caspase-1 activation and IL-1β secretion [127], and mononuclear cells from CAPS patients spontaneously secrete IL-1β and IL-18 [128], suggesting that these mutations generate a gain-of-function effect. Structural modeling of NLRP3 structure using NLRC4 as a template provides tantalizing clues to some of the disease-associated mutations.

Several different programs predict a strikingly similar structure for human NLRP3 with LRR removed (Fig. 10). As anticipated, most of the mutations map to NBD, HD1, and WHD, with a few in HD2. Many of the NLRP3 disease-associated mutations with high incidence are located at or close to the interface between NBD and WHD or HD2. These interface mutations likely disrupt auto-inhibition of NLRP3 by destabilizing the interactions among the subdomains. For example, the recurring mutation R260W that leads to inflammasome hyper-activation and consequently Th17-dominant inflammation in autoinflammatory diseases [129] affects Arg260, which is predicted to interact with residues from WHD. Mutation of Arg260 to the hydrophobic and bulky Trp is expected to disturb the NBD-WHD interaction, consequently activating NLRP3. Phe525 is located close to His522 (equivalent to His443 in Nlrc4), and the mutation F525L may cause local conformational changes that indirectly affect the interaction between ADP and its putative sensor His522 in NLRP3.

In addition to the interface mutations, there are a number of mutations that target the buried amino acids (Fig. 10). These buried mutations mostly map to the NBD, WHD and HD2 domains, and are predicted to perturb structural stability, thus attenuating inter-domain interactions and contributing to activation. Previous studies suggest that the gain-of-function mutations in mammalian and plant NLR proteins can be attributed to impairment of ATP hydrolysis in the mutant proteins [130,131]. Finally, a number of mutations map to the surface of NLRP3 (Fig. 10). These surface mutations may affect interactions with other proteins or block the oligomerization interface that is required for inflammasome formation. Although further biochemical

characterization of the disease-associated mutations is needed, this analysis strongly suggests that at least some mutations directly lead to relief of auto-inhibition and the constitutive activation of NLRP3, yielding uncontrolled production of IL-1β and IL-18.

PERSPECTIVE

Our understanding on the assembly of apoptosome and inflammasomes is far from complete. At present, the apoptosome complex involving Apaf-1, Dark or CED-4 has been successfully reconstituted using homogeneous recombinant proteins. The *in vitro* reconstitution of specific apoptosomes represents the first essential step in understanding the structure and functional mechanism of the apoptosomes. Kinetics and the regulation of the apoptosome assembly are only beginning to be investigated. The differential role of ATP/dATP in the assembly of various apoptosomes is yet to be scrutinized. The structure of the apoptosomes at an atomic resolution is expected to reveal critical insights into the assembly and mechanisms of the various apoptosomes. By sharp contrast to apoptosome, we have little understanding on the assembly of the inflammasomes.

Available experimental evidence suggests a common set of principles for the assembly of apoptosome and inflammasomes (Fig. 11). In the resting state, the scaffold protein—Apaf-1, Dark, or NLR—exists in an ADP-bound, auto-inhibited conformation. Such a closed conformation is maintained through extensive inter-domain interactions and stabilized by ADP. The binding of the activating ligand—cytochrome *c* for Apaf-1 and PAMP/DAMP for NLR—to the carboxyl-terminal ligand-sensing domain results in partial relief of auto-inhibition. Subsequently, the bound ADP is replaced by ATP, which triggers a major structural rearrangement to allow formation of the oligomeric apoptosome or inflammasome. It should be stated that, despite strong suspicion, nucleotide exchange has yet to be demonstrated for NLRs in the formation of inflammasomes.

By contrast to the central focus on the assembly of apoptosome and inflammasomes, little is known about the disassembly of such caspase-activating complexes—whether they can be disassembled, and if so, how disassembly is regulated. The fact that Apaf-1 exhibits a low level of ATPase activity strongly suggests that ATP hydrolysis may occur within the apoptosome, which could lead to

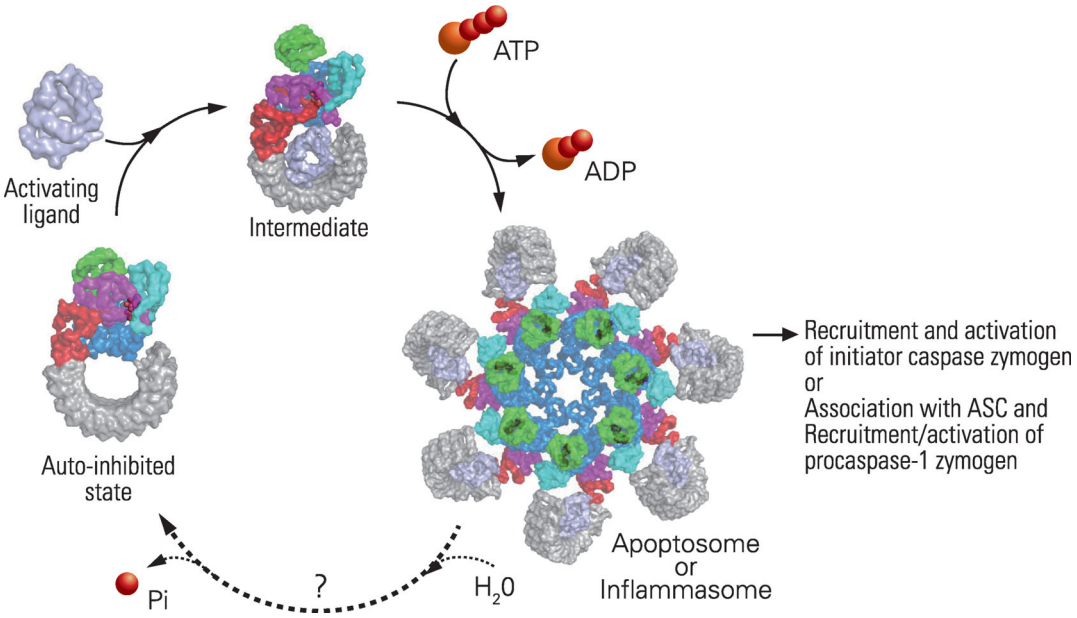

Figure 11. A general model for the assembly and disassembly of caspase-activating apoptosomes or inflammasomes. In the resting state, the scaffolding protein—Apaf-1 or NLR, exists in the ADP-bound, auto-inhibited state. Auto-inhibition is achieved by ADP-facilitated inter-domain interactions among NBD/HD1/WHD and incorrect positioning of the ligand-sensing domain (which impedes structural rearrangement required by oligomerization). Binding of the activating ligand results in conformational changes in the ligand-sensing domain (WD40 repeats in Apaf-1 and LRR in NLRs), lowering the barrier for further structural rearrangement. Replacement of ADP by ATP requires major structural rearrangement among NBD/HD1/WHD/HD2. Such rearrangement leads to the formation of an apoptosome or inflammasome. We speculate that ATP hydrolysis, or binding to a disassembly factor, may cause the disassembly of the apoptosome or inflammasome. The assembled apoptosome or inflammasome recruits the initiator caspase or additional adaptor proteins (ASC).

its disassembly (Fig. 11). There is a distinct possibility that ATP hydrolysis might be a general mechanism for the disassembly of apoptosome and inflammasomes.

The predominant purpose for the assembly of the multimeric apoptosome or inflammasome is to activate the initiator or inflammatory caspases, which are synthesized as inactive zymogens in the cell. Understanding the activation mechanism of initiator or inflammatory caspases requires comprehensive structural information and rigorous structure-guided biochemical characterization. Despite intense investigation of the past decade, there is only limited structural data on the apoptosome and scant information on the inflammasomes. As such, the detailed activation mechanism has yet to be convincingly elucidated for any initiator or inflammatory caspase. What we understand today may amount to the gross approximation of the hidden fact. This seemingly grim scenario embodies ample opportunity for research discoveries for many years to come.

FUNDING

This work was supported by grants from the National Natural Science Foundation of China and Ministry of Science and Technology of China.

REFERENCES

1. Danial, NN and Korsmeyer, SJ. Cell death: critical control points. *Cell* 2004; **116**: 205–19.
2. Horvitz, HR. Worms, life, and death (nobel lecture). *Chembiochem* 2003; **4**: 697–711.
3. Steller, H. Regulation of apoptosis in *Drosophila*. *Cell Death Differ* 2008; **15**: 1132–8.
4. Thornberry, NA and Lazebnik, Y. Caspases: enemies within. *Science* 1998; **281**: 1312–6.
5. Shi, Y. Mechanisms of caspase inhibition and activation during apoptosis. *Mol Cell* 2002; **9**: 459–70.
6. Degterev, A, Boyce, M and Yuan, J. A decade of caspases. *Oncogene* 2003; **22**: 8543–67.
7. Riedl, SJ and Shi, Y. Molecular mechanisms of caspase regulation during apoptosis. *Nature Review Mol Cell Biol* 2004; **5**: 897–907.
8. Thornberry, NA, Bull, HG and Calaycay, JR *et al.* A novel heterodimeric cysteine protease is required for interleukin-1 beta processing in monocytes. *Nature* 1992; **356**: 76874.
9. Cerreti, DP, Kozlosky, CJ and Mosley, B *et al.* Molecular cloning of the interleukin-1 beta converting enzyme. *Science* 1992; **256**: 97–100.
10. Fink, SL and Cookson, BT. Caspase-1-dependent pore formation during pyroptosis leads to osmotic lysis of infected host macrophages. *Cell Microbiol* 2005; **8**: 1812–25.
11. Fink, SL and Cookson, BT. Apoptosis, pyroptosis, and necrosis: mechanistic description of dead and dying eukaryotic cells. *Infect Immun* 2005; **73**: 1907–16.
12. Martinon, F and Tschopp, J. Inflammatory caspases and inflammasomes: master switches of inflammation. *Cell Death Differ* 2007; **14**: 10–22.
13. Yuan, J, Shaham, S and Ledoux, S *et al.* The *C. elegans* cell death gene Ced-3 encodes a protein similar to mammalian interleukin-1 beta-converting enzyme. *Cell* 1993; **75**: 641–52.
14. Xue, D, Shaham, S and Horvitz, HR. The *Caenorhabditis elegans* cell-death protein CED-3 is a cysteine protease with substrate specificities similar to those of the human CPP32 protease. *Genes Dev* 1996; **10**: 1073–83.
15. Denning, DP, Hatch, V and Horvitz, HR. Both the caspase CSP-1 and a caspase-independent pathway promote programmed cell death in parallel to the canonical pathway for apoptosis in *Caenorhabditis elegans*. *PLoS Genet* 2013; **9**: e1003341.
16. Salvesen, GS and Dixit, VM. Caspase activation: the induced-proximity model. *Proc Natl Acad Sci USA* 1999; **96**: 10964–7.
17. Chai, J, Wu, Q and Shiozaki, E *et al.* Crystal structure of a procaspase-7 zymogen: mechanisms of activation and substrate binding. *Cell* 2001; **107**: 399–407.
18. Riedl, SJ, Fuentes-Prior, P and Renatus, M *et al.* Structural basis for the activation of human procaspase-7. *Proc Natl Acad Sci USA* 2001; **98**: 14790–5.
19. Thomsen, ND, Koerber, JT and Wells, JA. Structural snapshots reveal distinct mechanisms of procaspase-3 and -7 activation. *Proc Natl Acad Sci USA* 2013; **110**: 8477–82.
20. Zou, H, Li, Y and Liu, X *et al.* An APAF-1-cytochrome *c* multimeric complex is a functional apoptosome that activates procaspase-9. *J Biol Chem* 1999; **274**: 11549–56.
21. Kischkel, FC, Hellbardt, S and Behrmann, I *et al.* Cytotoxicity-dependent APO-1 (Fas/CD95)-associated proteins form a death-inducing signaling complex (DISC) with the receptor. *EMBO J* 1995; **14**: 5579–88.
22. Srinivasula, SM, Poyet, JL and Razmara, M *et al.* The PYRIN-CARD protein ASC is an activating adaptor for caspase-1. *J Biol Chem* 2002; **277**: 21119–22.
23. Martinon, F, Burns, K and Tschopp, J. The inflammasome: a molecular platform triggering activation of inflammatory caspases and processing of proIL-beta. *Mol Cell* 2002; **10**: 417–26.
24. Stennicke, HR, Deveraux, QL and Humke, EW *et al.* Caspase-9 can be activated without proteolytic processing. *J Biol Chem* 1999; **274**: 8359–62.
25. Srinivasula, SM, Saleh, A and Hedge, R *et al.* A conserved XIAP-interaction motif in caspase-9 and Smac/DIABLO mediates opposing effects on caspase activity and apoptosis. *Nature* 2001; **409**: 112–6.
26. Hu, Q, Wu, D and Chen, W *et al.* Proteolytic processing of the caspase-9 zymogen is required for apoptosome-mediated activation of caspase-9. *J Biol Chem* 2013; **288**: 15142–7.
27. Acehan, D, Jiang, X and Morgan, DG *et al.* Three-dimensional structure of the apoptosome: Implications for assembly, procaspase-9 binding and activation. *Mol Cell* 2002; **9**: 423–32.

28. Saleh, A, Srinivasula, SM and Acharya, S *et al.* Cytochrome *c* and dATP-mediated oligomerization of Apaf-1 is a prerequisite for procaspase-9 activation. *J Biol Chem* 1999; **274**: 17941–5.
29. Hu, Y, Benedict, MA and Ding, L *et al.* Role of cytochrome *c* and dATP/ATP hydrolysis in Apaf-1-mediated caspase-9 activation and apoptosis. *EMBO J* 1999; **18**: 3586–95.
30. Rodriguez, J and Lazebnik, Y. Caspase-9 and Apaf-1 form an active holoenzyme. *Genes Dev* 1999; **13**: 3179–84.
31. Cain, K, Brown, DG and Langlais, C *et al.* Caspase activation involves the formation of the aposome, a large (∼700 kDa) caspase-activating complex. *J Biol Chem* 1999; **274**: 22686–92.
32. Rodriguez, A, Oliver, H and Zou, H *et al.* Dark is a *Drosophila* homologue of Apaf-1/CED-4 and functions in an evolutionarily conserved death pathway. *Nat Cell Biol* 1999; **1**: 272–9.
33. Zhou, L, Song, Z and Tittel, J *et al.* HAC-1, a *Drosophila* homolog of Apaf-1 and CED-4 functions in developmental and radiation-induced apoptosis. *Mol Cell* 1999; **4**: 745–55.
34. Kanuka, H, Sawamoto, K and Inohara, N *et al.* Control of the cell death pathway by Dapaf-1, a *Drosophila* Apaf-1/CED-4-related caspase activator. *Mol Cell* 1999; **4**: 757–69.
35. Yuan, J and Horvitz, HR. The *Caenorhabditis elegans* cell death gene ced-4 encodes a novel protein and is expressed during the period of extensive programmed cell death. *Development* 1992; **116**: 309–20.
36. Irmler, M, Hofmann, K and Vaux, D *et al.* Direct physical interaction between the *Caenorhabditis elegans* 'death proteins' CED-3 and CED-4. *FEBS Lett* 1997; **406**: 189–90.
37. Seshagiri, S and Miller, LK. *Caenorhabditis elegans* CED-4 stimulates CED-3 processing and CED-3-induced apoptosis. *Curr Biol* 1997; **7**: 455–60.
38. Chinnaiyan, AM, O'Rourke, K and Lane, BR *et al.* Interaction of CED-4 with CED-3 and CED-9: a molecular framework for cell death. *Science* 1997; **275**: 1122–6.
39. Wu, D, Wallen, HD and Nunez, G. Interaction and regulation of subcellular localization of CED-4 by CED-9. *Science* 1997; **275**: 1126–9.
40. Yang, X, Chang, HY and Baltimore, D. Essential role of CED-4 oligomerization in CED-3 activation and apoptosis. *Science* 1998; **281**: 1355–7.
41. Lamkanfi, M and Dixit, VM. Inflammasomes and their roles in health and disease. *Annu Rev Cell Dev Biol* 2012; **28**: 137–61.
42. von Moltke, J, Ayres, JS and Kofoed, EM. Chavarría-Smith J, RE V, recognition of bacteria by inflammasomes. *Annu Rev Immunol* 2013; **31**: 73–106.
43. Leipe, DD, Koonin, EV and Aravind, L. STAND, a class of P-loop NTPases including animal and plant regulators of programmed cell death: multiple, complex domain architectures, unusual phyletic patterns, and evolution by horizontal gene transfer. *J Mol Biol* 2004; **343**: 1–28.
44. Tinel, A and Tschopp, J. The PIDDosome, a protein complex implicated in activation of caspase-2 in response to genotoxic stress. *Science* 2004; **304**: 843–6.
45. Yuan, S and Akey, CW. Apoptosome structure, assembly, and procaspase activation. *Structure* 2013; **21**: 501–15.
46. Bratton, SB and Salvesen, GS. Regulation of the Apaf-1-caspase-9 apoptosome. *J Cell Sci* 2010; **123**: 3209–14.
47. Shi, Y. Apoptosome assembly. *Methods Enzymol* 2008; **442**: 141–56.
48. Liu, X, Kim, CN and Yang, J *et al.* Induction of apoptosis program in cell-free extracts: requirement for dATP and cytochrome *c*. *Cell* 1996; **86**: 147–57.
49. Zou, H, Henzel, WJ and Liu, X *et al.* Apaf-1, a human protein homologous to *C. elegans* CED-4, participates in cytochrome *c*-dependent activation of caspase-3. *Cell* 1997; **90**: 405–13.
50. Li, P, Nijhawan, D and Budihardjo, I *et al.* Cytochrome *c* and dATP-dependent formation of Apaf-1/caspase-9 complex initiates an apoptotic protease cascade. *Cell* 1997; **91**: 479–89.
51. Qin, H, Srinivasula, SM and Wu, G *et al.* Structural basis of procaspase-9 recruitment by the apoptotic protease-activating factor 1. *Nature* 1999; **399**: 547–55.
52. Benedict, MA, Hu, Y and Inohara, N *et al.* Expression and functional analysis of Apaf-1 isoforms. Extra Wd-40 repeat is required for cytochrome *c* binding and regulated activation of procaspase-9. *J Biol Chem* 2000; **275**: 8461–8.
53. Riedl, SJ, Li, W and Chao, Y. Schwarzenbacher R, Shi Y, structure of the apoptotic protease activating factor 1 bound to ADP. *Nature* 2005; **434**: 926–33.
54. Reubold, TF, Wohlgemuth, S and Eschenburg, S. Crystal structure of full-length Apaf-1: how the death signal is relayed in the mitochondrial pathway of apoptosis. *Structure* 2011; **19**: 1074–83.
55. Yuan, S, Yu, X and Topf, M *et al.* Structure of an apoptosome-procaspase-9 CARD complex. *Structure* 2010; **18**: 571–83.
56. Yu, X, Acehan, D and Menetret, JF *et al.* A structure of the human apoptosome at 12.8 A resolution provides insights into this cell death platform. *Structure* 2005; **13**: 1725–35.
57. Yuan, S, Yu, X and Asara, JM *et al.* The holo-apoptosome: activation of procaspase-9 and interactions with caspase-3. *Structure* 2011; **19**: 1084–96.
58. Bao, Q, Lu, W and Rabinowitz, JD *et al.* Calcium blocks formation of apoptosome by preventing nucleotide exchange in Apaf-1. *Mol Cell* 2007; **25**: 181–92.
59. Reubold, TF, Wohlgemuth, S and Eschenburg, S. A new model for the transition of APAF-1 from inactive monomer to caspase-activating apoptosome. *J Biol Chem* 2009; **284**: 32717–24.
60. Kim, HE, Du, F and Fang, M *et al.* Formation of apoptosome is initiated by cytochrome *c*-induced dATP hydrolysis and subsequent nucleotide exchange on Apaf-1. *Proc Natl Acad Sci USA* 2005; **102**: 17545–50.
61. Jiang, X, Kim, HE and Shu, H *et al.* Distinctive roles of PHAP proteins and prothymosin-alpha in a death regulatory pathway. *Science* 2003; **299**: 223–6.
62. Cain, K, Langlais, C and Sun, XM *et al.* Physiological concentrations of K+ inhibit cytochrome *c*-dependent formation of the apoptosome. *J Biol Chem* 2001; **276**: 41985–90.
63. Karki, P, Seong, C and Kim, JE *et al.* Intracellular K(+) inhibits apoptosis by suppressing the Apaf-1 apoptosome formation and subsequent downstream pathways but not cytochrome *c* release. *Cell Death Differ* 2007; **14**: 2068–75.
64. Chandra, D, Bratton, SB and Person, MD *et al.* Intracellular nucleotides act as critical prosurvival factors by binding to cytochrome *c* and inhibiting apoptosome. *Cell* 2006; **125**: 1333–46.
65. Chereau, D, Zou, H and Spada, AP *et al.* A nucleotide binding site in caspase-9 regulates apoptosome activation. *Biochemistry* 2005; **44**: 4971–6.
66. Boatright, KM and Salvesen, GS. Mechanisms of caspase activation. *Curr Opin Cell Biol* 2003; **15**: 725–31.
67. Renatus, M, Stennicke, HR and Scott, FL *et al.* Dimer formation drives the activation of the cell death protease caspase 9. *Proc Natl Acad Sci USA* 2001; **98**: 14250–5.
68. Pop, C, Timmer, J and Sperandio, S *et al.* The apoptosome activates caspase-9 by dimerization. *Mol Cell* 2006; **22**: 269–75.
69. Walker, NP, Talanian, RV and Brady, KD *et al.* Crystal structure of the cysteine protease interleukin-1b-converting enzyme: a (p20/p10)2 homodimer. *Cell* 1994; **78**: 343–52.
70. Wilson, KP, Black, J-A and Thomson, JA *et al.* Structure and mechanism of interleukin-1b converting enzyme. *Nature* 1994; **370**: 270–5.

71. Rotonda, J, Nicholson, DW and Fazil, KM *et al.* The three-dimensional structure of apopain/CPP32, a key mediator of apoptosis. *Nat Struct Biol* 1996; **3**: 619–25.
72. Yin, Q, Park, HH and Chung, JY *et al.* Caspase-9 holoenzyme is a specific and optimal procaspase-3 processing machine. *Mol Cell* 2006; **22**: 259–68.
73. Shi, Y. Caspase activation: revisiting the induced proximity model. *Cell* 2004; **117**: 855–8.
74. Chao, Y, Shiozaki, EN and Srinivasula, SM *et al.* Engineering a dimeric caspase-9: a re-evaluation of the induced proximity model for caspase activation. *PLoS Biol* 2005; **3**: e183.
75. Dorstyn, L, Colussi, PA and Quinn, LM *et al.* DRONC, an ecdysone-inducible *Drosophila* caspase. *Proc Natl Acad Sci USA* 1999; **96**: 4307–12.
76. Chew, SK, Akdemir, F and Chen, P *et al.* The apical caspase Dronc governs programmed and unprogrammed cell death in *Drosophila*. *Dev Cell* 2004; **7**: 897–907.
77. Daish, TJ, Mills, K and Kumar, S. Drosophila caspase DRONC is required for specific developmental cell death pathways and stress-induced apoptosis. *Dev Cell* 2004; **7**: 909–15.
78. Muro, I, Monser, K and Clem, RJ. Mechanism of Dronc activation in *Drosophila* cells. *J Cell Sci* 2004; **117**: 5035–41.
79. Yu, X, Wang, L and Acehan, D *et al.* Three-dimensional structure of a double apoptosome formed by the *Drosophila* Apaf-1 related killer. *J Mol Biol* 2006; **355**: 577–89.
80. Diemand, AV and Lupas, AN. Modeling AAA + ring complexes from monomeric structures. *J Struct Biol* 2006; **156**(1): 230–43.
81. Yuan, S, Yu, X and Topf, M *et al.* Structure of the *Drosophila* apoptosome at 6.9 Å resolution. *Structure* 2011; **19**: 128–40.
82. Dorstyn, L and Kumar, S. A biochemical analysis of the activation of the *Drosophila* caspase DRONC. *Cell Death Differ* 2008; **15**: 461–70.
83. Snipas, SJ, Drag, M and Stennicke, HR *et al.* Activation mechanism and substrate specificity of the *Drosophila* initiator caspase DRONC. *Cell Death Differ* 2008; **15**: 938–45.
84. Yan, N, Huh, JR and Schirf, V *et al.* Structure and activation mechanism of the *Drosophila* initiator caspase Dronc. *J Biol Chem* 2006; **281**: 8667–74.
85. Horvitz, HR. Genetic control of programmed cell death in the nematode *Caenorhabditis elegans*. *Cancer Res* 1999; **59**: 1701–6.
86. Hengartner, MO and Horvitz, HR. *C. elegans* cell survival gene ced-9 encodes a functional homolog of the mammalian proto-oncogene bcl-2. *Cell* 1994; **76**: 665–76.
87. Chen, F, Hersh, BM and Conradt, B *et al.* Translocation of *C. elegans* CED-4 to nuclear membranes during programmed cell death. *Science* 2000; **287**: 1485–9.
88. James, C, Gschmeissner, S and Fraser, A *et al.* CED-4 induces chromatin condensation in Schizosaccharomyces pombe and is inhibited by direct physical association with CED-9. *Curr Biol* 1997; **7**: 246–52.
89. Spector, MS, Desnoyers, S and Hoeppner, DJ *et al.* Interaction between the *C. elegans* cell-death regulators CED-9 and CED-4. *Nature* 1997; **385**: 653–6.
90. Conradt, B and Horvitz, HR. The *C. elegans* protein EGL-1 is required for programmed cell death and interacts with the Bcl-2-like protein CED-9. *Cell* 1998; **93**: 519–29.
91. del Peso, L, Gonzalez, VM and Nunez, G. *Caenorhabditis elegans* EGL-1 disrupts the interaction of CED-9 with CED-4 and promotes CED-3 activation. *J Biol Chem* 1998; **273**: 33495–500.
92. del Peso, L, Gonzalez, VM and Inohara, N *et al.* Disruption of the CED-9.CED-4 complex by EGL-1 is a critical step for programmed cell death in *Caenorhabditis elegans*. *J Biol Chem* 2000; **275**: 27205–11.
93. Parrish, J, Metters, H and Chen, L *et al.* Demonstration of the *in vivo* interaction of key cell death regulators by structure-based design of second-site suppressors. *Proc Natl Acad Sci USA* 2000; **97**: 11916–21.
94. Yan, N, Chai, J and Lee, ES *et al.* Structure of the CED-4-CED-9 complex provides insights into programmed cell death in *Caenorhabditis elegans*. *Nature* 2005; **437**: 831–7.
95. Yan, N, Xu, Y and Shi, Y. 2:1 Stoichiometry of the CED-4-CED-9 Complex and the tetrameric CED-4: insights into the regulation of CED-3 activation. *Cell Cycle* 2006; **5**: 31–4.
96. Yan, N, Gu, L and Kokel, D *et al.* Structural, biochemical, functional analyses of CED-9 recognition by the proapoptotic proteins EGL-1 and CED-4. *Mol Cell* 2004; **15**: 999–1006.
97. Qi, S, Pang, Y and Hu, Q *et al.* Crystal structure of the *Caenorhabditis elegans* apoptosome reveals an octameric assembly of CED-4. *Cell* 2010; **141**: 446–57.
98. Huang, W, Jiang, T and Choi, W *et al.* Mechanistic insights into CED-4-mediated activation of CED-3. *Genes Dev* 2013. In press.
99. Hu, Z, Yan, C and Liu, P *et al.* Crystal structure of NLRC4 reveals its autoinhibition mechanism. *Science* 2013; **341**: 172–5.
100. Poyet, JL, Srinivasula, SM and Tnani, M *et al.* Identification of Ipaf, a human caspase-1-activating protein related to Apaf-1. *J Biol Chem* 2001; **276**: 28309–13.
101. Kofoed, EM and Vance, RE. Innate immune recognition of bacterial ligands by NAIPs determines inflammasome specificity. *Nature* 2011; **477**: 592–5.
102. Danot, O, Marquenet, E and Vidal-Ingigliardi, D *et al.* Wheel of life, wheel of death: a mechanistic insight into signaling by STAND proteins. *Structure* 2009; **17**: 172–82.
103. Erzberger, JP and Berger, JM. Evolutionary relationships and structural mechanisms of AAA+ proteins. *Annu Rev Biophys Biomol Struct* 2006; **35**: 93–114.
104. Rossman, KL, Der, CJ and Sondek, J. GEF means go: turning on RHO GTPases with guanine nucleotide-exchange factors. *Nat Rev Mol Cell Biol* 2005; **6**: 167–80.
105. Bendahmane, A, Farnham, G and Moffett, P *et al.* Constitutive gain-of-function mutants in a nucleotide binding site-leucine rich repeat protein encoded at the Rx locus of potato. *Plant J* 2002; **32**: 195–204.
106. de la Fuente van Bentem, S, Vossen, JH and de Vries, KJ *et al.* Heat shock protein 90 and its co-chaperone protein phosphatase 5 interact with distinct regions of the tomato I-2 disease resistance protein. *Plant J* 2005; **43**: 284–98.
107. Howles, P, Lawrence, G and Finnegan, J *et al.* Autoactive alleles of the flax L6 rust resistance gene induce non-race-specific rust resistance associated with the hypersensitive response. *Mol Plant Microbe In* 2005; **18**: 570–82.
108. Gabriels, SH, Vossen, JH and Ekengren, SK *et al.* An NB-LRR protein required for HR signalling mediated by both extra- and intracellular resistance proteins. *Plant J* 2007; **50**: 14–28.
109. Faustin, B, Lartigue, L and Bruey, JM *et al.* Reconstituted NALP1 inflammasome reveals two-step mechanism of caspase-1 activation. *Mol Cell* 2007; **25**: 713–24.
110. Halff, EF, Diebolder, CA and Versteeg, M *et al.* Formation and structure of a NAIP5-NLRC4 inflammasome induced by direct interactions with conserved N- and C-terminal regions of flagellin. *J Biol Chem* 2012; **287**: 38460–72.
111. Cassel, SL, Joly, S and Sutterwala, FS. The NLRP3 inflammasome: a sensor of immune danger signals. *Semin Immunol* 2009; **21**: 194–1981.
112. Bryant, C and Fitzgerald, KA. Molecular mechanisms involved in inflammasome activation. *Trends Cell Biol* 2009; **19**: 455–64.
113. Tschopp, J and Schroder, K. NLRP3 inflammasome activation: the convergence of multiple signalling pathways on ROS production? *Nat Rev Immunol* 2010; **10**: 210–5.

114. Wen, H, Miao, EA and Ting, JP. Mechanisms of NOD-like receptor-associated inflammasome activation. *Immunity* 2013; **39**: 432–41.
115. Nakahira, K, Haspel, JA and Rathinam, VA *et al.* Autophagy proteins regulate innate immune responses by inhibiting the release of mitochondrial DNA mediated by the NALP3 inflammasome. *Nat Immunol* 2011; **12**: 222–30.
116. Zhou, R, Yazdi, AS and Menu, P *et al.* A role for mitochondria in NLRP3 inflammasome activation. *Nature* 2011; **469**: 221–5.
117. Subramanian, N, Natarajan, K and Clatworthy, MR *et al.* The adaptor MAVS promotes NLRP3 mitochondrial localization and inflammasome activation. *Cell* 2013; **153**: 348–61.
118. Iyer, SS, He, Q and Janczy, JR *et al.* Mitochondrial cardiolipin is required for nlrp3 inflammasome activation. *Immunity* 2013; **39**: 311–23.
119. Strowig, T, Henao-Mejia, J and Elinav, E *et al.* Inflammasomes in health and disease. *Nature* 2012; **481**: 278–86.
120. Davis, BK, Wen, H and Ting, JP. The inflammasome NLRs in immunity, inflammation, and associated diseases. *Annu Rev Immunol* 2011; **29**: 707–35.
121. Hoffman, HM, Mueller, JL and Broide, DH *et al.* Mutation of a new gene encoding a putative pyrin-like protein causes familial cold autoinflammatory syndrome and Muckle-Wells syndrome. *Nat Genet* 2001; **29**: 301–5.
122. Feldmann, J, Prieur, AM and Quartier, P *et al.* Chronic infantile neurological cutaneous and articular syndrome is caused by mutations in CIAS1, a gene highly expressed in polymorphonuclear cells and chondrocytes. *Am J Hum Genet* 2002; **71**: 198–203.
123. Aksentijevich, I, Nowak, M and Mallah, M *et al.* *De novo* CIAS1 mutations, cytokine activation, and evidence for genetic heterogeneity in patients with neonatal-onset multisystem inflammatory disease (NOMID): a new member of the expanding family of pyrin-associated autoinflammatory diseases. *Arthritis Rheum* 2002; **46**: 3340–8.
124. Masters, SL, Simon, A and Aksentijevich, I *et al.* Horror autoinflammaticus: the molecular pathophysiology of autoinflammatory disease (*). *Annu Rev Immunol* 2009; **27**: 621–68.
125. Stojanov, S and Kastner, DL. Familial autoinflammatory diseases: genetics, pathogenesis and treatment. *Curr Opin Rheumatol* 2005; **17**: 586–99.
126. Hull, KM, Shoham, N and Chae, JJ *et al.* The expanding spectrum of systemic autoinflammatory disorders and their rheumatic manifestations. *Curr Opin Rheumatol* 2003; **15**: 61–9.
127. Duncan, JA, Bergstralh, DT and Wang, Y *et al.* Cryopyrin/NALP3 binds ATP/dATP, is an ATPase, and requires ATP binding to mediate inflammatory signaling. *Proc Natl Acad Sci USA* 2007; **104**: 8041–6.
128. Dowds, TA, Masumoto, J and Zhu, L *et al.* Cryopyrin-induced interleukin 1beta secretion in monocytic cells: enhanced activity of disease-associated mutants and requirement for ASC. *J Biol Chem* 2004; **279**: 21924–8.
129. Meng, G, Zhang, F and Fuss, I *et al.* A mutation in the Nlrp3 gene causing inflammasome hyperactivation potentiates Th17 cell-dominant immune responses. *Immunity* 2009; **30**: 860–74.
130. Neven, B, Callebaut, I and Prieur, AM *et al.* Molecular basis of the spectral expression of CIAS1 mutations associated with phagocytic cell-mediated autoinflammatory disorders CINCA/NOMID, MWS, and FCU. *Blood* 2004; **103**: 2809–15.
131. Tameling, WI, Vossen, JH and Albrecht, M *et al.* Mutations in the NB-ARC domain of I-2 that impair ATP hydrolysis cause autoactivation. *Plant Physiol* 2006; **140**: 1233–45.
132. Hiller, S, Kohl, A and Fiorito, F *et al.* NMR structure of the apoptosis- and inflammation-related NALP1 pyrin domain. *Structure* 2003; **11**: 1199–1205.
133. DeLano, WL. The PyMOL molecular graphics system. http://www.pymol.org, 2002.